addenda and errata

Hydrated metal(II) complexes of N-(6-amino-3,4-dihydro-3-methyl-5-nitroso-4-oxopyrimidin-2-yl) derivatives of glycine, glycylglycine, threonine, serine, valine and methionine: a monomeric complex and coordination polymers in one, two and three dimensions linked by hydrogen bonding. Corrigendum

M. Luz Godino Salido,[a] Paloma Arranz Mascarós,[a] Rafaél López Garzón,[a] M. Dolores Gutiérrez Valero,[a] John N. Low,[b] John F. Gallagher[c] and Christopher Glidewell[d]*

[a]Departamento de Química Inorgánica y Orgánica, Universidad de Jaén, 23071 Jaén, Spain, [b]Department of Chemistry, University of Aberdeen, Meston Walk, Old Aberdeen, AB24 3UE, Scotland, [c]School of Chemical Sciences, Dublin City University, Dublin 9, Ireland, and [d]School of Chemistry, University of St Andrews, St Andrews KY16 9ST, Scotland

Correspondence e-mail: cg@st-andrews.ac.uk

Some of the data collection details for compound (VIII) were incorrectly given in Table 1 of Godino Salido *et al.* (2004). The data for compound VIII in this paper were collected using synchrotron radiation at the Daresbury SRS station 9.8, $\lambda = 0.6935$ Å (Cernik *et al.*, 1997; Clegg, 2000). The data were collected using a Bruker SMART 1K CCD diffractometer using ω rotation with narrow frames. The computer program used in the data collection was *SMART* (Bruker, 2001) and for cell refinement and data reduction *SAINT* (Bruker, 2001).

References

Bruker (2001). *SAINT* and *SMART*. AXS Inc., Madison, Wisconsin, USA.
Cernik, R. J., Clegg, W., Catlow, C. R. A., Bushnell-Wye, G., Flaherty, J. V., Greaves, G. N., Hamichi, M., Burrows, I., Taylor D. J. & Teat, S. J. (1997). *J. Synchrotron Rad.* **4**, 279–286; **7**, 40.
Clegg, W. (2000). *J. Chem. Soc. Dalton Trans.* pp. 3223–3232.
Godino Salido, M. L., Arranz Mascarós, P., López Garzón, R., Gutiérrez Valero, M. D., Low, J. N., Gallagher, J. F. & Glidewell, C. (2004). *Acta Cryst.* **B60**, 46–64.

Hydrated metal(II) complexes of N-(6-amino-3,4-dihydro-3-methyl-5-nitroso-4-oxopyrimidin-2-yl) derivatives of glycine, glycylglycine, threonine, serine, valine and methionine: a monomeric complex and coordination polymers in one, two and three dimensions linked by hydrogen bonding

M. Luz Godino Salido,[a] Paloma Arranz Mascarós,[a] Rafaél López Garzón,[a] M. Dolores Gutiérrez Valero,[a] John N. Low,[b]‡ John F. Gallagher[c] and Christopher Glidewell[d]*

[a]Departamento de Química Inorgánica y Orgánica, Universidad de Jaén, 23071 Jaén, Spain, [b]Department of Chemistry, University of Aberdeen, Meston Walk, Old Aberdeen, AB24 3UE, Scotland, [c]School of Chemical Sciences, Dublin City University, Dublin 9, Ireland, and [d]School of Chemistry, University of St Andrews, St Andrews KY16 9ST, Scotland

‡ Postal address: Department of Electronic Engineering and Physics, University of Dundee, Nethergate, Dundee DD1 4HN, Scotland.

Correspondence e-mail: cg@st-andrews.ac.uk

Nine hydrated complexes of Group 2 (alkaline earth) cations with organic ligands which are N-substituted amino acids containing the 6-amino-3,4-dihydro-3-methyl-5-nitroso-4-oxopyrimidin-2-yl group have been structurally characterized. The octahydrated calcium glycinate complex, where the six-coordinate Ca cation lies on an inversion centre in the space group $P\bar{1}$, forms a finite (zero-dimensional) complex. The hexahydrated barium glycinate complex contains eight-coordinate Ba and it is isostructural with the known Sr analogue, and its one-dimensional coordination polymer takes the form of a simple chain. The octahydrated calcium and strontium threonine complexes are isostructural, with eight-coordinate cations lying on twofold rotation axes in the space group $C2$: the one-dimensional coordination polymers take the form of a chain of spiro-fused rings and a similar chain of spiro-fused rings is found in the heptahydrated barium serine complex, although here the ten-coordinate cation lies in a general position. In the tetrahydrated strontium and barium glycylglycinate complexes, the eight-coordinate cations lie on twofold rotation axes in the space group $C2/c$, but in the Sr complex the coordination polymer is a chain of spiro-fused rings, while in the Ba complex the coordination polymer forms deeply puckered sheets. There are two types of Ca site in the hexahydrated calcium valine complex: one is eight coordinate and gives rise to a two-dimensional coordination polymer, while the other is seven coordinate forming a finite, zero-dimensional coordination complex. In the heptahydrated barium methionine complex, the coordination polymer is three dimensional. In all of the complexes, the coordination aggregates are further linked by an extensive series of hydrogen bonds.

1. Introduction

The potassium(I) salt of the substituted glycinate anion L^A [see Scheme (I)] crystallizes as a monohydrate $K(L^A)\cdot H_2O$ (Low, Moreno Sánchez et al., 2001), and the supramolecular structure takes the form of an organic–inorganic hybrid sheet in which metal–oxygen ribbons are linked by strips containing only organic ligands. The metal–oxygen ribbon contains vertex-sharing octahedra, while the nitroso group of the anion acts as an η^2 ligand towards K^+. The sodium(I) salt of L^A, of the composition $[Na_2(L^A)_2(H_2O)_3]$, also forms a hybrid structure, but here the metal–oxygen ribbon contains edge-

Table 1
Experimental details.

	I	II	III	IV	V
Crystal data					
Chemical formula	$C_{14}H_{24}Ca$-$N_{10}O_{12}\cdot4H_2O$	$C_{14}H_{26}Ba$-$N_{10}O_{13}\cdot H_2O$	$C_{18}H_{28}Ca$-$N_{10}O_{12}\cdot4H_2O$	$C_{18}H_{28}N_{10}$-$O_{12}Sr\cdot4H_2O$	$C_{16}H_{28}Ba$-$N_{10}O_{14}\cdot3H_2O$
M_r	636.58	697.79	688.65	736.19	775.45
Cell setting, space group	Triclinic, $P\bar{1}$	Monoclinic, $P2_1/c$	Monoclinic, $C2$	Monoclinic, $C2$	Triclinic, $P1$
a, b, c (Å)	7.4540 (7), 7.6148 (11), 12.5939 (17)	24.9613 (4), 6.91570 (10), 14.6427 (2)	30.2259 (11), 6.4043 (2), 7.3667 (3)	30.6420 (5), 6.4888 (1), 7.3733 (1)	7.1387 (2), 7.4974 (2), 13.5644 (4)
α, β, γ (°)	95.850 (6), 97.040 (8), 110.038 (8)	90.00, 93.1490 (10), 90.00	90.00, 94.610 (2), 90.00	90.00, 94.4319 (9), 90.00	99.5040 (9), 94.3080 (10), 99.6000 (16)
V (Å^3)	658.52 (14)	2523.88 (6)	1421.40 (9)	1461.65 (4)	702.05 (3)
Z	1	4	2	2	1
D_x (Mg m^{-3})	1.605	1.836	1.609	1.673	1.834
Radiation type	Mo $K\alpha$	Mo $K\alpha$	Mo $K\alpha$	Mo $K\alpha$	Mo $K\alpha$
No. of reflections for cell parameters	2833	5709	3182	3314	5818
θ range (°)	2.9–27.0	3.0–27.5	3.0–27.4	3.0–27.5	2.9–27.4
μ (mm^{-1})	0.33	1.66	0.32	1.94	1.51
Temperature (K)	120 (2)	120 (2)	120 (2)	120 (2)	120 (2)
Crystal form, colour	Lath, pink	Plate, yellow	Plate, pink	Block, red	Plate, pink
Crystal size (mm)	$0.10 \times 0.07 \times 0.01$	$0.42 \times 0.36 \times 0.08$	$0.24 \times 0.24 \times 0.04$	$0.70 \times 0.50 \times 0.25$	$0.40 \times 0.26 \times 0.02$
Data collection					
Diffractometer	Kappa-CCD	Kappa-CCD	Kappa-CCD	Kappa-CCD	Kappa-CCD
Data collection method	ϕ scans, and ω scans with κ offsets	ϕ scans, and ω scans with κ offsets	ϕ scans, and ω scans with κ offsets	ϕ scans, and ω scans with κ offsets	ϕ scans, and ω scans with κ offsets
Absorption correction	Multi-scan	Multi-scan	Multi-scan	Multi-scan	Multi-scan
T_{min}	0.963	0.548	0.867	0.331	0.625
T_{max}	0.998	0.881	0.990	0.618	0.970
No. of measured, independent and observed reflections	5368, 2833, 1311	26 202, 5709, 5255	9010, 3182, 2469	9899, 3314, 3291	10 911, 5818, 5773
Criterion for observed reflections	$I > 2\sigma(I)$	$I > 2\sigma(I)$	$I > 2\sigma(I)$	$I > 2\sigma(I)$	$I > 2\sigma(I)$
R_{int}	0.103	0.074	0.073	0.062	0.038
θ_{max} (°)	27.0	27.5	27.4	27.5	27.4
Range of h, k, l	$-9 \Rightarrow h \Rightarrow 9$ $-9 \Rightarrow k \Rightarrow 9$ $-16 \Rightarrow l \Rightarrow 16$	$-32 \Rightarrow h \Rightarrow 32$ $-8 \Rightarrow k \Rightarrow 8$ $-18 \Rightarrow l \Rightarrow 18$	$-38 \Rightarrow h \Rightarrow 38$ $-8 \Rightarrow k \Rightarrow 8$ $-9 \Rightarrow l \Rightarrow 9$	$-39 \Rightarrow h \Rightarrow 39$ $-8 \Rightarrow k \Rightarrow 8$ $-9 \Rightarrow l \Rightarrow 9$	$-9 \Rightarrow h \Rightarrow 9$ $-9 \Rightarrow k \Rightarrow 9$ $-17 \Rightarrow l \Rightarrow 17$
Refinement					
Refinement on	F^2	F^2	F^2	F^2	F^2
$R[F^2 > 2\sigma(F^2)]$, $wR(F^2)$, S	0.057, 0.150, 0.90	0.078, 0.208, 1.19	0.049, 0.096, 1.02	0.028, 0.069, 1.04	0.030, 0.075, 1.01
No. of reflections	2833	5739	3182	3314	5818
No. of parameters	188	354	206	209	397
H-atom treatment	Constrained to parent site	Constrained to parent site	Constrained to parent site	Constrained to parent site	Constrained to parent site
Weighting scheme	$w = 1/[\sigma^2(F_o^2) + (0.0574P)^2]$, where $P = (F_o^2 + 2F_c^2)/3$	$w = 1/[\sigma^2(F_o^2) + 84.2219P]$, where $P = (F_o^2 + 2F_c^2)/3$	$w = 1/[\sigma^2(F_o^2) + (0.0339P)^2]$, where $P = (F_o^2 + 2F_c^2)/3$	$w = 1/[\sigma^2(F_o^2) + (0.030P)^2 + 1.5757P]$, where $P = (F_o^2 + 2F_c^2)/3$	$w = 1/[\sigma^2(F_o^2) + (0.0297P)^2 + 0.7753P]$, where $P = (F_o^2 + 2F_c^2)/3$
$(\Delta/\sigma)_{max}$	<0.0001	0.001	<0.0001	<0.0001	<0.0001
$\Delta\rho_{max}$, $\Delta\rho_{min}$ (e Å^{-3})	0.39, -0.51	3.61, -4.21	0.30, -0.33	0.33, -0.46	0.44, -0.93
Extinction method	None	None	None	$SHELXL$	None
Extinction coefficient	–	–	–	0.0164 (8)	–
Absolute structure	–	–	Flack (1983), 1412 Friedel pairs	Flack (1983), 1486 Friedel pairs	Flack (1983), 2609 Friedel pairs
Flack parameter	–	–	-0.08 (5)	-0.017 (4)	-0.006 (12)

	VI	VII	VIII	IX
Crystal data				
Chemical formula	$C_{18}H_{30}N_{12}O_{14}Sr$	$C_{18}H_{30}BaN_{12}O_{14}$	$C_{20}H_{36}CaN_{10}O_{12}\cdot C_{20}H_{38}Ca$ $N_{10}O_{13}\cdot3.123H_2O$	$C_{20}H_{36}BaN_{10}O_{12}S_2$-$\cdot3H_2O$
M_r	726.16	775.87	1371.37	864.11
Cell setting, space group	Monoclinic, $C2/c$	Monoclinic, $C2/c$	Monoclinic, $P2_1$	Tetragonal, $P4_3$
a, b, c (Å)	12.9517 (3), 7.7020 (2), 26.5416 (7)	13.3918 (3), 7.4669 (2), 28.8211 (7)	7.5557 (3), 13.9726 (6), 29.4179 (12)	21.6978 (2), 21.6978 (2), 7.40570 (10)

Table 1 (continued)

|	VI	VII	VIII	IX
β ($^\circ$)	97.2770 (12)	103.1310 (10)	91.803 (2)	90.00
V (Å^3)	2626.30 (11)	2806.62 (12)	3104.2 (2)	3486.56 (7)
Z	4	4	2	4
D_x (Mg m^{-3})	1.837	1.836	1.467	1.646
Radiation type	Mo $K\alpha$	Mo $K\alpha$	Mo $K\alpha$	Mo $K\alpha$
No. of reflections for cell parameters	2982	3148	14 077	7394
θ range ($^\circ$)	3.1–27.5	3.1–27.4	2.0–29.2	3.0–27.5
μ (mm^{-1})	2.15	1.51	0.28	1.34
Temperature (K)	120 (2)	120 (2)	120 (2)	120 (2)
Crystal form, colour	Plate, purple	Plate, pink	Plate, pink	Plate, pink
Crystal size (mm)	0.25 × 0.25 × 0.06	0.20 × 0.15 × 0.04	0.05 × 0.04 × 0.03	0.60 × 0.03 × 0.02
Data collection				
Diffractometer	Kappa-CCD	Kappa-CCD	Kappa-CCD	Kappa-CCD
Data collection method	ϕ scans, and ω scans with κ offsets	ϕ scans, and ω scans with κ offsets	ϕ scans, and ω scans with κ offsets	ϕ scans, and ω scans with κ offsets
Absorption correction	Multi-scan	Multi-scan	Multi-scan	Multi-scan
$T_{\min}$	0.616	0.753	0.967	0.501
$T_{\max}$	0.882	0.942	0.992	0.974
No. of measured, independent and observed reflections	16 348, 2982, 2369	7598, 3148, 2905	21 417, 14 077, 13 181	21 371, 7394, 7035
Criterion for observed reflections	$I > 2\sigma(I)$	$I > 2\sigma(I)$	$I > 2\sigma(I)$	$I > 2\sigma(I)$
R_{int}	0.073	0.046	0.027	0.072
$\theta_{\max}$ ($^\circ$)	27.5	27.4	29.2	27.5
Range of h, k, l	$-12 \Rightarrow h \Rightarrow 16$	$-17 \Rightarrow h \Rightarrow 8$	$-10 \Rightarrow h \Rightarrow 7$	$-28 \Rightarrow h \Rightarrow 23$
	$-9 \Rightarrow k \Rightarrow 9$	$-9 \Rightarrow k \Rightarrow 8$	$-18 \Rightarrow k \Rightarrow 17$	$-28 \Rightarrow k \Rightarrow 26$
	$-34 \Rightarrow l \Rightarrow 34$	$-37 \Rightarrow l \Rightarrow 37$	$-40 \Rightarrow l \Rightarrow 41$	$-9 \Rightarrow l \Rightarrow 7$
Refinement				
Refinement on	F^2	F^2	F^2	F^2
$R[F^2 > 2\sigma(F^2)]$, $wR(F^2)$, S	0.049, 0.134, 1.04	0.034, 0.085, 1.24	0.037, 0.085, 1.05	0.036, 0.089, 1.05
No. of reflections	2982	3148	14 077	7394
No. of parameters	205	205	888	478
H-atom treatment	Constrained to parent site	Constrained to parent site	Constrained to parent site	Constrained to parent site
Weighting scheme	$w = 1/[\sigma^2(F_o^2) + (0.0779P)^2 + 5.4996P]$, where $P = (F_o^2 + 2F_c^2)/3$	$w = 1/[\sigma^2(F_o^2)P)^2 + 16.8531P]$, where $P = (F_o^2 + 2F_c^2)/3$	$w = 1/[\sigma^2(F_o^2) + (0.0407P)^2 + 0.4491P]$, where $P = (F_o^2 + 2F_c^2)/3$	$w = 1/[\sigma^2(F_o^2) + (0.0289P)^2 + 4.0203P]$, where $P = (F_o^2 + 2F_c^2)/3$
$(\Delta/\sigma)_{\max}$	<0.0001	0.001	0.003	0.001
$\Delta\rho_{\max}$, $\Delta\rho_{\min}$ (e Å^{-3})	1.43, −0.74	0.99, −0.84	0.40, −0.39	0.74, −0.71
Extinction method	None	None	None	None
Absolute structure	–	–	Flack (1983), 5320 Friedel pairs	Flack (1983), 3077 Friedel pairs
Flack parameter			0.085 (17)	−0.022 (13)

Computer programs used: *Kappa-CCD server software* (Nonius, 1997), *DENZO-SMN* (Otwinowski & Minor, 1997), *SHELXS*97 (Sheldrick, 1997b), *SHELXL*97 (Sheldrick, 1997a); *PLATON* (Spek, 2003); *PRPKAPPA* (Ferguson, 1999).

shared trigonal bipyramids and the nitroso group of the anion acts as an η^1 ligand towards Na$^+$. The lithium(I) and manganese(II) salts of L^A form finite complexes, [Li(L^A)(H$_2$O)$_3$] and [Mn(L^A)$_2$(H$_2$O)$_4$]·6H$_2$O, which are linked into three-dimensional frameworks by an extensive series of hydrogen bonds, while the strontium(II) complex [Sr(L^A)$_2$(H$_2$O)$_5$]·H$_2$O forms a one-dimensional coordination polymer (Glidewell *et al.*, 2002). By contrast, in the magnesium(II) (Arranz Mascarós *et al.*, 2000) and the zinc(II) (Arranz Mascarós *et al.*, 1999) salts of L^A there is no coordination of L^A to the metal centre, and both have constitutions [M(H$_2$O)$_6$](L^A)$_2$·2H$_2$O.

The analogous glycylglycinate anion L^B [see Scheme (I)] forms hydrated complexes with potassium(I) and calcium(II), [K(L^B)(H$_2$O)] (Low, Arranz, Cobo, Fontecha, Godino, López & Glidewell, 2001) and [Ca(L^B)$_2$(H$_2$O)$_3$] (Low, Arranz, Cobo,

Fontecha, Godino, López, Cannon *et al.*, 2001), whose supramolecular structures take the form of coordination polymers in three dimensions and one dimension, respectively, differing markedly from the supramolecular structures generated using the simpler ligand L^A.

Intrigued by these structural differences, we have now initiated a study of the supramolecular structures of salts and complexes formed by a range of Group 2 cations with a range of ligands analogous to L^A and L^B, synthesized in many cases from enantiopure chiral amino acids [see Scheme (I)]. We may note here that any organic inorganic hybrid materials formed by chiral analogues of L^A or L^B must necessarily crystallize in non-centrosymmetric space groups, so fulfilling one of the requirements for non-linear optical behaviour (Masse *et al.*, 1999; Muthuraman *et al.*, 1999).

(I)
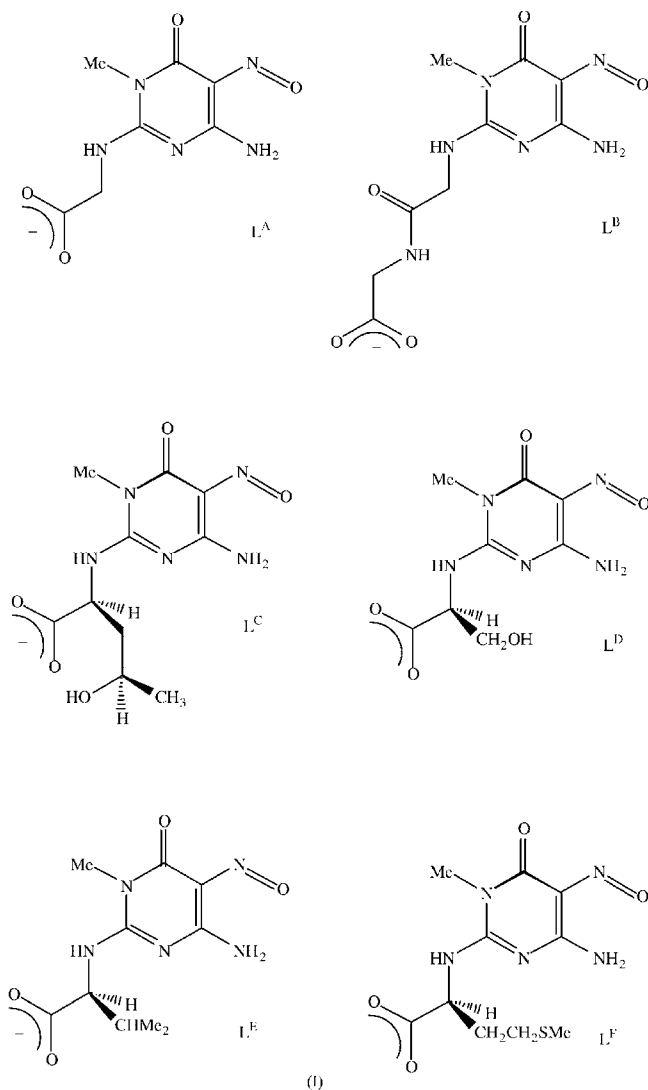
This paper reports on the molecular and supramolecular structures of the following nine hydrated complexes: the Ca and Ba complexes of the ligand L^A, compounds (1) and (2), respectively, the latter of which proves to be isostructural with the Sr analogue reported earlier (Glidewell *et al.*, 2002); the Ca and Sr complexes of the ligand L^C, compounds (3) and (4), respectively; the Ba complex of L^D, compound (5); the Sr and Ba complexes of L^B, compounds (6) and (7), respectively; the Ca complex of L^E, compound (8); and the Ba complex of ligand L^F, compound (9). The overall compositions of these complexes are as follows: (1) $[Ca(L^A)_2 \cdot 8H_2O]$; (2) $[Ba(L^A)_2 \cdot 6H_2O]$; (3) and (4), $[M(L^C)_2 \cdot 6H_2O]$ (M = Ca, Sr); (5), $[Ba(L^D)_2 \cdot 7H_2O]$; (6) and (7), $[M(L^B)_2 \cdot 4H_2O]$ (M = Sr, Ba); (8), $[Ca(L^E)_2 \cdot 6H_2O]$; and (9) $[Ba(L^F)_2 \cdot 7H_2O]$.

2. Experimental

2.1. Synthesis

Neutral (*N*-pyrimidyl)amino acids corresponding to the anionic ligands L^A–L^F [see Scheme (I)] were prepared using the methods described previously (Low *et al.*, 2000).

Compound (1): Equimolar quantities (0.5 mmol) of calcium chloride dihydrate and tetramethylammonium *N*-(6-amino-3,4-dihydro-3-methyl-5-nitroso-4-oxopyrimidin-2-yl)glycinate were separately dissolved in water. The solutions were mixed and the resulting pink precipitate was filtered off. Slow evaporation of the filtrate gave pink crystals of (1), which were collected by filtration. Analysis: found C 26.5, H 5.2, N 21.8%; $C_{14}H_{32}CaN_{10}O_{16}$ requires C 26.4, H 5.1, N 22.0%.

Compound (2): Equimolar quantities (0.5 mmol) of barium chloride dihydrate and tetramethylammonium *N*-(6-amino-3,4-dihydro-3-methyl-5-nitroso-4-oxopyrimidin-2-yl)glycinate were separately dissolved in water. The solutions were mixed and the mixture was allowed to crystallize at room temperature, providing pink crystals of (2), which were collected by filtration and washed with ethanol. Analysis: found C 24.1, H 4.2, N 20.0%; $C_{14}H_{28}BaN_{10}O_{14}$ requires C 24.1, H 4.1, N 20.3%.

Compound (3): Calcium chloride dihydrate (0.5 mmol) was added to a solution of *N*-(6-amino-3,4-dihydro-3-methyl-5-nitroso-4-oxopyrimidin-2-yl)threonine (0.5 mmol) in water (40 cm^3). Slow evaporation of the mixture yielded pink crystals of (3), which were collected by filtration and washed with ethanol. Analysis: found C 31.4, H 5.4, N 20.3%; $C_{18}H_{36}CaN_{10}O_{16}$ requires: C 31.4, H 5.3, N 20.3%.

Compound (4): Strontium chloride hexahydrate (0.5 mmol) was added to a solution of *N*-(6-amino-3,4-dihydro-3-methyl-5-nitroso-4-oxopyrimidin-2-yl)threonine (0.5 mmol) in water (40 cm^3). Slow evaporation of the mixture yielded pink crystals of (4), which were collected by filtration and washed with ethanol. Analysis: found C 29.3, H 5.2, N 18.9%; $C_{18}H_{36}N_{10}O_{16}Sr$ requires: C 29.4, H 4.9, N 19.0%.

Compound (5): Equimolar quantities (0.5 mmol) of KOH and *N*-(6-amino-3,4-dihydro-3-methyl-5-nitroso-4-oxopyrimidin-2-yl)serine were dissolved in water (10 cm^3), and a solution of barium chloride dihydrate (0.50 mmol) dissolved in water (20 cm^3) was added. The resulting precipitate was filtered off and the filtrate was then allowed to evaporate. After 2 d, pink tabular crystals of (5) were collected by filtration and washed with ethanol. Analysis: found: C 25.8, H 4.7, N 18.8%; $C_{16}H_{34}BaN_{10}O_{17}$ requires: C 24.8, H 4.4, N 18.1%.

Compound (6): To a hot solution (60 cm^3) of tetramethylammonium chloride in water (0.25 mol dm^{-3}) was added strontium hydroxide (0.35 mmol) followed by *N*-(6-amino-3,4-dihydro-3-methyl-5-nitroso-4-oxopyrimidin-2-yl)-glycylglycine (0.35 mmol). Slow evaporation of the pink solution obtained yielded, after 5 d at room temperature, purple crystals of (6), which were collected by filtration and then washed with cold water and ethanol. Analysis: found C 29.3, H 4.0, N 22.3%; $C_{18}H_{30}N_{12}O_{14}Sr$ requires C 29.8, H 4.2, N 23.2%.

Compound (7): Equimolar quantities (0.35 mmol) of barium hydroxide and *N*-(6-amino-3,4-dihydro-3-methyl-5-nitroso-4-oxopyrimidin-2-yl)glycylglycine were separately dissolved in water. When the solutions were mixed an orange precipitate was produced and filtered off. The resulting pink solution was then slowly evaporated at room temperature

research papers

giving, after 5 d, pink crystals of (7), which were collected by filtration and then washed with ethanol and ether. Analysis: found C 28.6, H 4.1, N 22.1%; $C_{18}H_{30}BaN_{12}O_{14}$ requires C 27.8, H 3.9, N 21.7%.

Compound (8): *N*-(6-Amino-3,4-dihydro-3-methyl-5-nitroso-4-oxopyrimidin-2-yl)valine (0.5 mmol) was mixed with 5 cm^3 of an aqueous solution of tetramethylammonium hydroxide (0.1 mol dm^{-3}) and this was then added to a solution of calcium chloride dihydrate (0.5 mmol) in water (20 cm^3). The resulting solution was reduced in volume and after several days gave a mixture of pink and colourless crystals: these were collected by filtration, washed with ethanol and then separated manually to provide pink tabular crystals of (8). Analysis: found C 35.1, H 6.2, N 20.2%; $C_{20}H_{40}CaN_{10}O_{14}$ requires: C 35.1, H 5.9, N 20.5%.

Compound (9): Equimolar quantities (0.5 mmol) of *N*-(6-amino-3,4-dihydro-3-methyl-5-nitroso-4-oxopyrimidin-2-yl)-methionine and KOH were dissolved in water (10 cm^3) and a solution of barium chloride dihydrate (0.50 mmol) dissolved in water (20 cm^3) was added. Slow evaporation of the resultant solution yielded pink crystals of (9), which were collected by filtration and washed with ethanol. Analysis: found C 28.9, H 4.9, N 16.3, S 7.2%; $C_{20}H_{42}BaN_{10}O_{17}S_2$ requires: C 27.8, H 4.9, N 16.2, S 7.4%.

Crystals suitable for single-crystal X-ray diffraction were in every case selected directly from the samples as prepared.

2.2. Data collection, structure solution and refinement

Details of cell data, data collection and structure solution and refinement are summarized in Table 1. Compound (1) is triclinic: the space group $P\bar{1}$ was chosen and confirmed by the analysis. For (2) the space group $P2_1/c$ was uniquely assigned
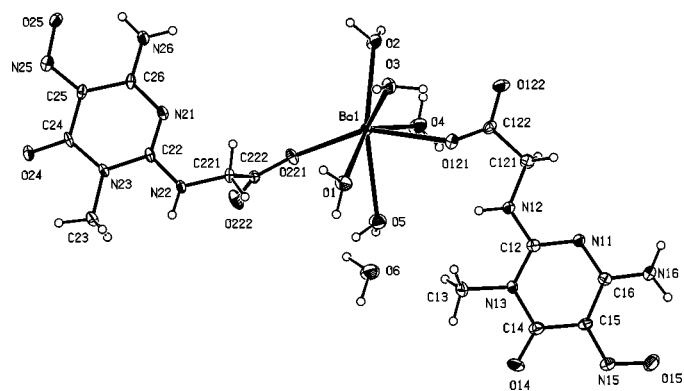

Figure 1
The independent components of (1) showing the octahedral coordination of the Ca and the atom-labelling scheme. Displacement ellipsoids are drawn at the 30% probability level. The atoms marked 'a' are at the symmetry position $(1-x, 1-y, 1-z)$ and the Ca1 atom has 0.5 occupancy.

Figure 2
The independent components of (2) showing the atom-labelling scheme. Displacement ellipsoids are drawn at the 30% probability level.
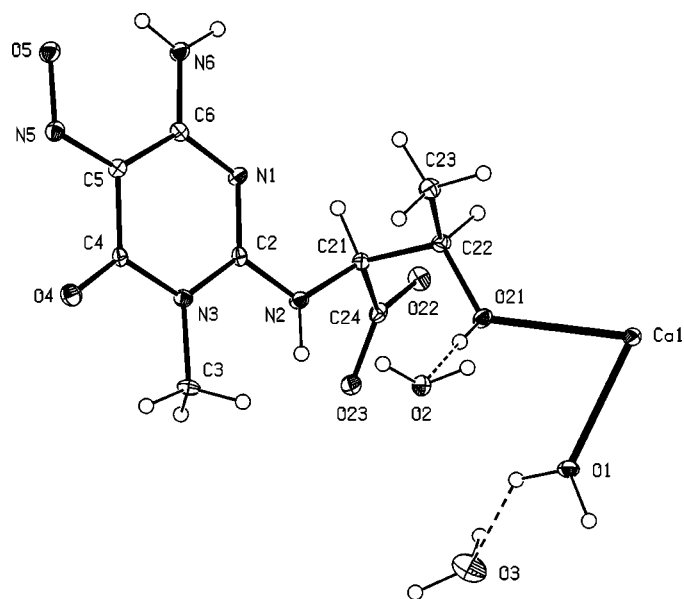

Figure 3
The independent components of (3) showing the atom-labelling scheme. Displacement ellipsoids are drawn at the 30% probability level and the Ca1 atom has 0.5 occupancy.

Table 2
Metal–oxygen distances (Å).

(1)†			
Ca1—O121	2.263 (3)	Ca1—O1	2.363 (3)
		Ca1—O2	2.379 (3)
(2)			
Ba1—O121	2.656 (8)	Ba1—O1	2.752 (8)
Ba1—O221	2.765 (7)	Ba1—O2	2.762 (7)
Ba1—O25^i	2.837 (7)	Ba1—O3	2.866 (8)
		Ba1—O4	2.802 (8)
		Ba1—O5	2.771 (8)
(3)‡			
Ca1—O21	2.473 (2)	Ca1—O1	2.395 (2)
Ca1—O22^{ii}	2.437 (2)		
Ca1—O23^{ii}	2.605 (2)		
(4)‡			
Sr1—O21	2.611 (2)	Sr1—O1	2.535 (2)
Sr1—O22^{ii}	2.591 (2)		
Sr1—O23^{ii}	2.704 (2)		
(5)			
Ba1—O11	2.912 (3)	Ba1—O1	2.773 (3)
Ba1—O12	2.859 (3)	Ba1—O2	2.695 (3)
Ba1—O13^{iii}	2.787 (3)	Ba1—O3	2.903 (3)
Ba1—O21	2.765 (3)	Ba1—O4	2.980 (3)
Ba1—O23^{iii}	2.815 (3)	Ba1—O5	3.238 (4)
(6)‡			
Sr1—O21	2.547 (2)	Sr1—O1	2.598 (3)
Sr1—O23^{ii}	2.618 (2)	Sr1—O2	2.502 (3)
(7)‡			
Ba1—O21	2.762 (2)	Ba1—O1	2.767 (3)
Ba1—O23^{iv}	2.816 (2)	Ba1—O2	2.808 (3)
(8)			
Ca1—O121	2.403 (2)	Ca1—O1	2.363 (2)
Ca1—O221	2.403 (2)	Ca1—O2	2.512 (2)
Ca1—O15^v	2.510 (2)	Ca1—O3	2.399 (2)
Ca1—O25^{vi}	2.685 (2)	Ca1—O4	2.455 (2)
Ca2—O321	2.385 (2)	Ca2—O5	2.369 (2)
Ca2—O421	2.345 (2)	Ca2—O6	2.430 (2)
		Ca2—O7	2.441 (2)
		Ca2—O8	2.369 (2)
		Ca2—O9	2.522 (2)
(9)			
Ba1—O11	2.756 (3)	Ba1—O1	2.829 (3)
Ba1—O21	2.747 (3)	Ba1—O2	2.909 (3)
Ba1—O25^{vii}	3.299 (3)	Ba1—O3	2.894 (3)
		Ba1—O4	2.888 (3)
		Ba1—O1^{viii}	2.826 (3)
		Ba1—O2^{viii}	2.815 (3)
		Ba1—O3^{viii}	2.915 (3)

Symmetry codes: (i) $1 - x, \frac{1}{2} + y, \frac{1}{2} - z$; (ii) $x, -1 + y, z$; (iii) $1 + x, y, z$; (iv) $\frac{1}{2} + x, \frac{1}{2} + y, z$; (v) $-x, -\frac{1}{2} + y, 1 - z$; (vi) $1 - x, \frac{1}{2} + y, 1 - z$; (vii) $y, 1 - x, \frac{1}{4} + z$; (viii) $2 - x, 1 - y, \frac{1}{2} + z$. † M lies at a centre of inversion. ‡ M lies on a twofold rotation axis.

from the systematic absences. For the isostructural compounds (3) and (4) the systematic absences permitted the space groups $C2$, Cm and $C2/m$, and for (8) the systematic absences permitted the space groups $P2_1$ and $P2_1/m$; in view of the chiral nature of the ligands, the space groups $C2$ and $P2_1$ were selected and confirmed by the successful structure solution and refinement. Compound (5) is triclinic and the space group $P1$ was chosen on the basis of the ligand chirality and
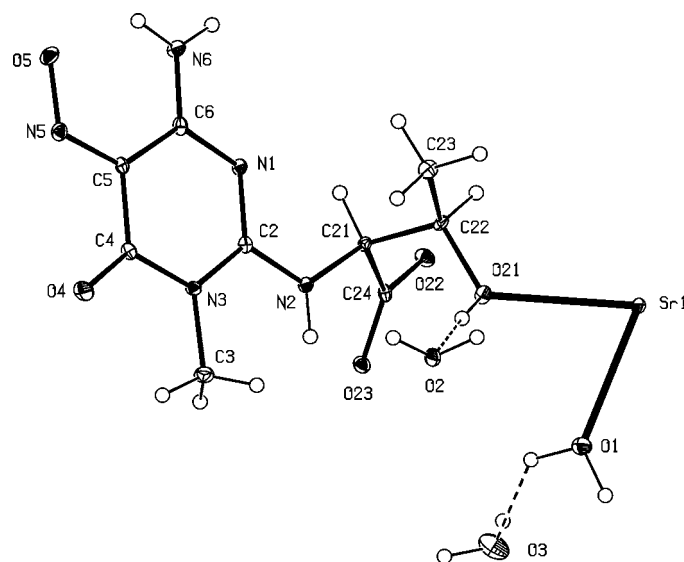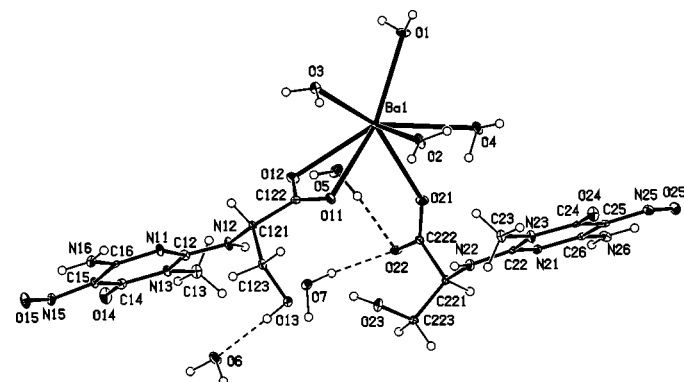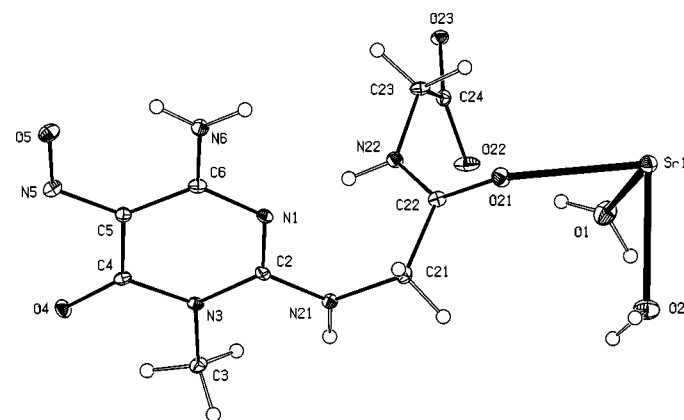

Figure 4
The independent components of (4) showing the atom-labelling scheme. Displacement ellipsoids are drawn at the 30% probability level and the Sr1 atom has 0.5 occupancy.

Figure 5
The independent components of (5) showing the atom-labelling scheme. Displacement ellipsoids are drawn at the 30% probability level.

Figure 6
The independent components of (6) showing the atom-labelling scheme. Displacement ellipsoids are drawn at the 30% probability level and the Sr1 atom has 0.5 occupancy.

confirmed by the successful structure solution and refinement. For (6) and (7) the systematic absences permitted the space groups Cc and $C2/c$. In each case the space group $C2/c$ was selected and confirmed by the successful structure solution and refinement. For (9) the systematic absences permitted the unique assignment of one member of the enantiomorphous pair of space groups $P4_1$ and $P4_3$. The space group $P4_3$ was selected by reference to the known configuration of the enantiopure amino acid component and confirmed by the value of the Flack parameter (Flack, 1983), -0.022 (13) for 3077 Friedel pairs. For (3), (4), (5) and (8) the absolute configurations were set by reference to the known amino acid configurations and confirmed by the values of the Flack parameters, -0.08 (5), -0.017 (4), -0.006 (12) and 0.085 (17) for 1412, 1486, 2609 and 45 320 Friedel pairs, respectively.

The structures were all solved by direct methods using *SHELXS*97 (Sheldrick, 1997a) and refined on F^2 with all data using *SHELXL*97 (Sheldrick, 1997b). A weighting scheme based upon $P = [F_o^2 + 2F_c^2]/3$ was employed in order to reduce statistical bias (Wilson, 1976). All H atoms were located from difference maps and all were included in the refinements as riding atoms. In (8) two of the four independent isopropyl fragments in the side chains, those pendent from C121 and C321, were found to be disordered: in each case the disorder was modelled using two sets of sites: for the fragments connected to C121 the refined values of the site-occupancy factors were 0.722 (7) and 0.278 (7), while for those bonded to C321 they were 0.880 (6) and 0.120 (6), respectively. It is probable that the occupancy of these disordered fragments is correlated to some extent, in order to avoid the occurrence of unacceptably short non-bonded contacts between C atoms in the two side chains. Compound (8) also contains a partially occupied water site O1S, with occupancy 0.123 (8), but no H atoms associated with this site could be located. In (9) the terminal $-\mathrm{CH_2SCH_3}$ unit of the type 1 ligand (containing N11 *etc.*) was found to be very heavily disordered. This fragment was modelled using three sets of sites; isotropic refinement led to site-occupancy factors of 0.390, 0.270 and 0.340, which were thereafter fixed at these values during the final anisotropic refinement.

Supramolecular analyses were made and the diagrams were prepared with the aid of *PLATON* (Spek, 2003). Figs. 1–30 show the independent components of (1)–(9) with the atom-labelling schemes and aspects of their supramolecular structures. Selected molecular dimensions are given in Tables 2 and 3, and details of the hydrogen bonding are in Table 4.[1]

3. Results and discussion

3.1. Constitutions and metal coordination

The calcium salt (1) of the substituted glycinate anion L^A has the same gross composition $[M(L^A)_2\cdot8\mathrm{H_2O}]$ as the Mg and Zn analogues (Arranz Mascarós *et al.*, 1999, 2000), but it

---

[1] Supplementary data for this paper are available from the IUCr electronic archives (Reference: NA5011). Services for accessing these data are described at the back of the journal.

---

differs from these latter two derivatives in that the two anions are coordinated directly to the Ca ion *via* their carboxylate groups in monodentate fashion, with the centrosymmetric octahedral coordination around Ca being completed by four water molecules (Fig. 1). Hence the overall constitution of (1) is $[M(L^A)_2\cdot(\mathrm{H_2O})_4]\cdot4\mathrm{H_2O}$, as opposed to $[M(\mathrm{H_2O})_6]$-
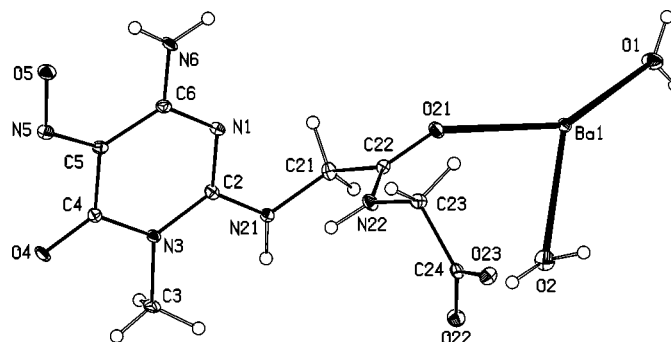

Figure 7
The independent components of (7) showing the atom-labelling scheme. Displacement ellipsoids are drawn at the 30% probability level and the Ba1 atom has 0.5 occupancy.
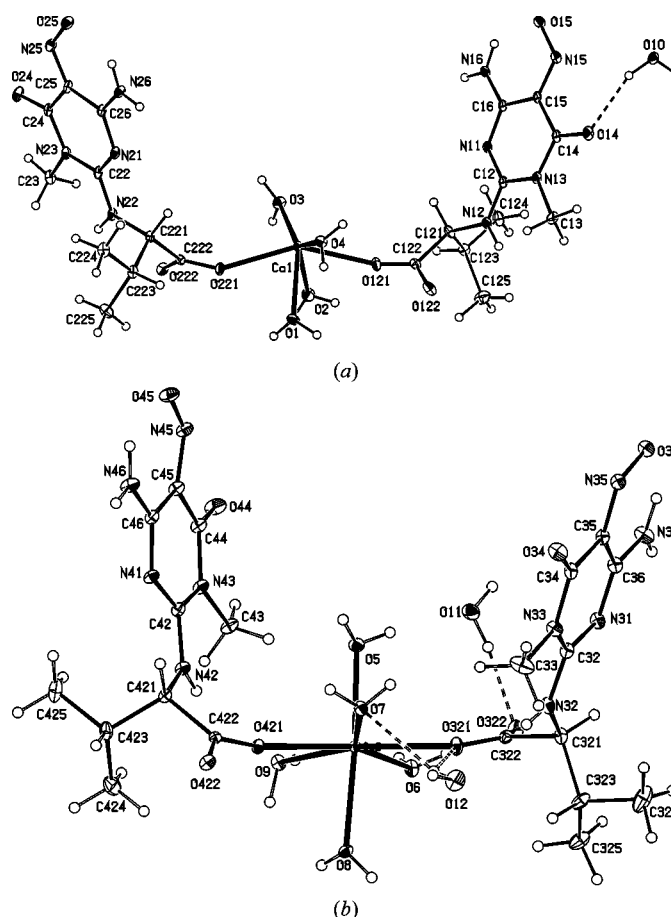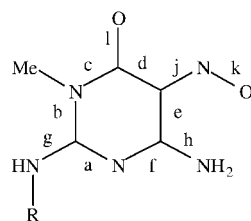
(a)

(b)

Figure 8
The independent components of (8) showing the atom-labelling scheme: (*a*) Ca1 and its ligands; (*b*) Ca2 and its ligands, together in each case with the hydrogen-bonded water molecules. The partially occupied water O1S has been omitted. Displacement ellipsoids are drawn at the 30% probability level.

Table 3
Selected bond lengths for (1)–(9) (Å).

a	b	c	d	e	f	g	h	j	k	l	Δ
(1)											
1.321 (5)	1.377 (4)	1.386 (5)	1.451 (5)	1.430 (5)	1.336 (5)	1.331 (5)	1.323 (5)	1.335 (5)	1.296 (4)	1.227 (4)	0.039
(2)†											
1.346 (12)	1.363 (13)	1.402 (13)	1.446 (15)	1.440 (13)	1.350 (12)	1.321 (12)	1.320 (13)	1.334 (12)	1.285 (12)	1.227 (13)	0.049
1.308 (12)	1.414 (11)	1.390 (12)	1.451 (13)	1.457 (12)	1.325 (13)	1.329 (12)	1.323 (13)	1.323 (12)	1.293 (11)	1.240 (11)	0.030
(3)											
1.323 (3)	1.380 (3)	1.395 (3)	1.458 (3)	1.440 (3)	1.344 (3)	1.341 (3)	1.320 (3)	1.343 (3)	1.298 (3)	1.221 (3)	0.045
(4)											
1.323 (3)	1.379 (3)	1.405 (3)	1.454 (3)	1.451 (3)	1.343 (3)	1.342 (2)	1.308 (3)	1.343 (3)	1.289 (3)	1.220 (3)	0.054
(5)‡											
1.330 (7)	1.384 (5)	1.382 (6)	1.456 (6)	1.447 (6)	1.344 (8)	1.318 (7)	1.317 (7)	1.343 (7)	1.293 (6)	1.225 (6)	0.050
1.327 (5)	1.381 (5)	1.394 (9)	1.468 (8)	1.443 (6)	1.346 (6)	1.328 (6)	1.318 (6)	1.334 (8)	1.291 (7)	1.225 (8)	0.041
(6)											
1.337 (4)	1.377 (4)	1.395 (4)	1.464 (5)	1.439 (5)	1.338 (4)	1.326 (4)	1.326 (4)	1.342 (4)	1.291 (4)	1.228 (4)	0.051
(7)											
1.333 (4)	1.386 (4)	1.393 (4)	1.451 (5)	1.444 (5)	1.334 (5)	1.331 (4)	1.321 (4)	1.346 (5)	1.289 (4)	1.230 (4)	0.057
(8)§											
1.333 (2)	1.388 (2)	1.393 (3)	1.460 (3)	1.446 (3)	1.340 (3)	1.330 (3)	1.326 (3)	1.351 (3)	1.280 (2)	1.241 (3)	0.071
1.325 (3)	1.385 (2)	1.408 (3)	1.449 (3)	1.455 (3)	1.344 (3)	1.340 (3)	1.321 (3)	1.347 (3)	1.278 (3)	1.235 (3)	0.069
1.332 (3)	1.391 (3)	1.395 (3)	1.453 (3)	1.452 (3)	1.341 (3)	1.333 (3)	1.321 (3)	1.344 (3)	1.291 (2)	1.234 (3)	0.053
1.326 (3)	1.392 (3)	1.406 (3)	1.455 (3)	1.447 (3)	1.347 (3)	1.341 (3)	1.324 (3)	1.347 (3)	1.281 (3)	1.225 (3)	0.066
(9)¶											
1.330 (6)	1.381 (5)	1.399 (5)	1.455 (6)	1.426 (6)	1.354 (5)	1.334 (5)	1.308 (6)	1.349 (5)	1.285 (5)	1.225 (6)	0.064
1.330 (5)	1.380 (5)	1.397 (5)	1.441 (6)	1.435 (6)	1.340 (5)	1.328 (5)	1.316 (6)	1.354 (5)	1.268 (5)	1.237 (5)	0.086

$\Delta = (j - k)$.　† Two independent anionic ligands, see Fig. 2.　‡ Two independent anionic ligands, see Fig. 5.　§ Four independent anionic ligands, see Fig. 8.　¶ Two independent anionic ligands, see Fig. 9.

$(L^A)_2 \cdot 2H_2O$ for the Mg and Zn analogues. The Ba complex (2) of the ligand L^A, $[Ba(L^A)_2 \cdot 6H_2O]$ (Fig. 2), is isostructural with the Sr analogue (Glidewell *et al.*, 2002). The Ba cation is eight-coordinate, taking the form of a distorted square antiprism in which five of the six water molecules are directly linked to the metal, while the coordination is completed by two carboxyl groups, both monodentate, and one nitrosyl O atom: the two independent anions thus differ in their coordination behaviour. The structures reported here for (1) and (2) bring to six the number of hydrated M^{II} complexes of the ligand L^A which have now been structurally characterized, and four of these contain the Group 2 metals Mg, Ca, Sr and Ba, the first two of which crystallize as octahydrates and the last two as hexahydrates. While both the Mg and Ca complexes contain six-coordinate metals, only the larger Ca has the anionic ligands

coordinated, whereas the complexes of the large cations Sr and Ba contain eight-coordinate metals.

In the two isomorphous hexahydrates (3) and (4) (Figs. 3 and 4), the Ca and Sr cations lie on twofold rotation axes in the space group $C2$ and are eight-coordinate, as opposed to the six-coordination of Ca in (1). The coordination polyhedron is made up of two carboxylate groups each binding to the cation in bidentate fashion, two hydroxyl O from the threonine side chains and two water molecules (Table 2): the four remaining water molecules are linked to coordinated O *via* O—H···O hydrogen bonds (Table 4). In the heptahydrate (5) (Fig. 5), all components lie in general positions and the barium cation is ten-coordinate. This ten-coordination is made up of five water molecules, one of which (containing O5) is rather weakly bound although also linked into the asymmetric unit *via* a

hydrogen bond, together with five coordinating O from the anionic ligands: one monodentate carboxylate, one bidentate carboxylate and the two unionized hydroxyl groups in the serine side chain. Two further water molecules are linked to the rest of the structure via O—H···O hydrogen bonds.

The Sr and Ba derivatives of the glycylglycinate anion L^B, (6) and (7), respectively, both crystallize as tetrahydrates (Figs. 6 and 7): by contrast, the Ca analogue crystallizes as a trihy-
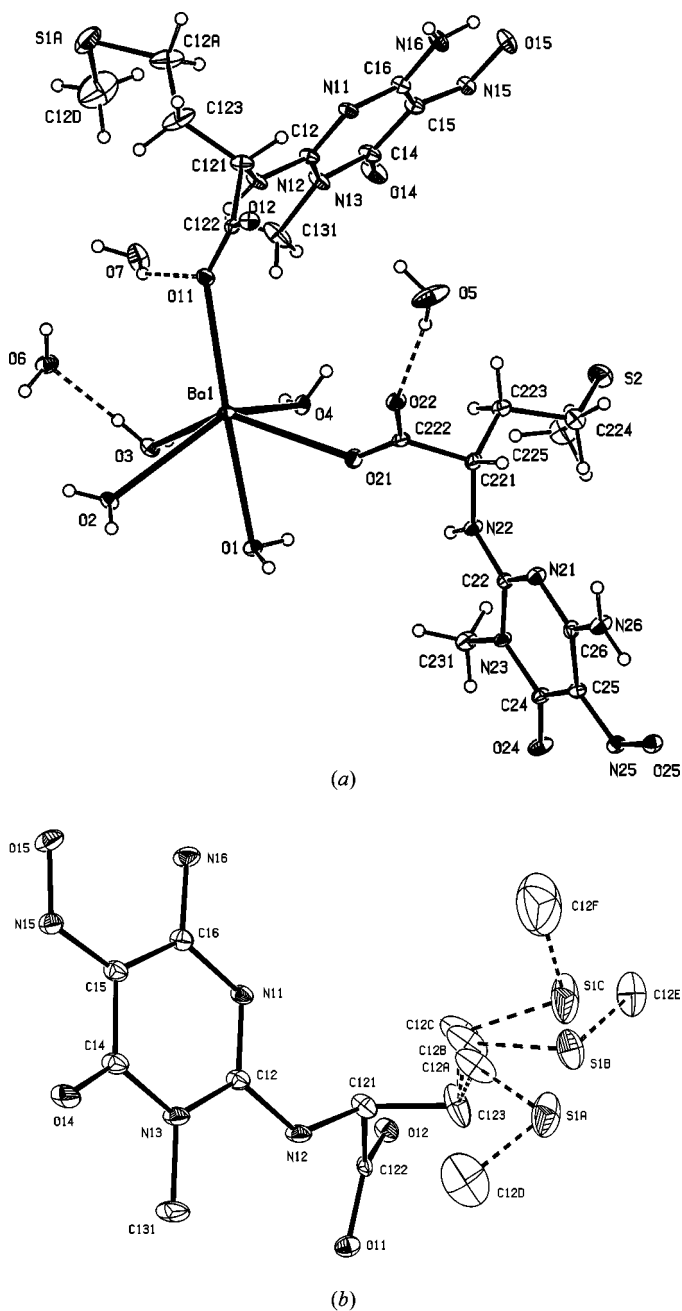

(a)

(b)

Figure 9
The independent components of (9) showing the atom-labelling scheme: (a) for the sake of clarity showing only one component of the disordered anion and (b) the disordered anion only, showing all of the components (see text). Displacement ellipsoids are drawn at the 30% probability level.
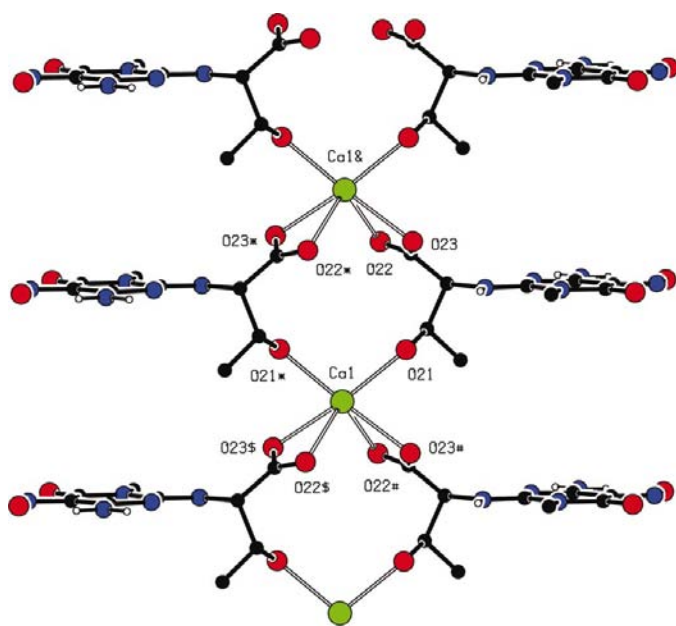
Figure 10
Part of the crystal structure of (3) showing the formation of a one-dimensional coordination polymer along [010]. For the sake of clarity, the water molecules, the H atoms bonded to C atoms and the unit-cell box are all omitted. The atoms marked with an asterisk (*), a hash (#) or a dollar sign ($) are at the symmetry positions $(2 - x, y, 1 - z)$, $(x, -1 + y, z)$ and $(2 - x, -1 + y, 1 - z)$, respectively, and atom Ca1& is at the position $(1, 1 + y, \frac{1}{2})$.
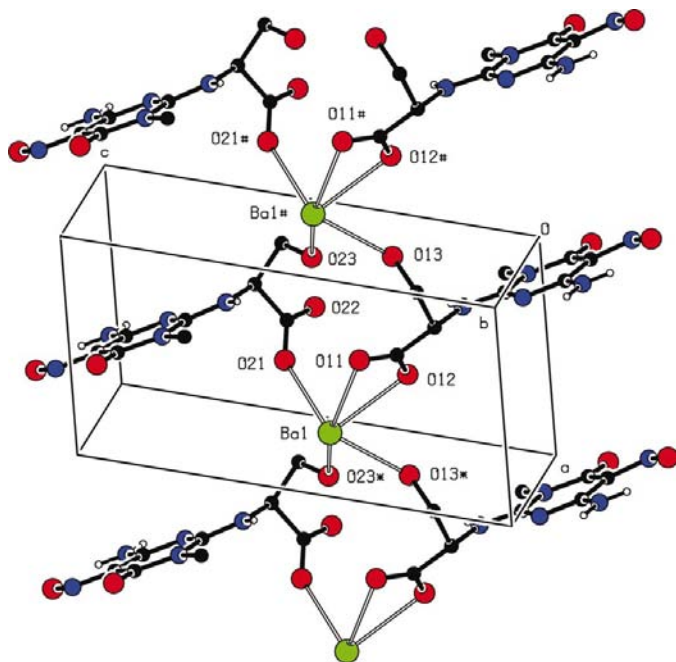
Figure 11
Part of the crystal structure of (5) showing the formation of a one-dimensional coordination polymer along [100]. For the sake of clarity, the water molecules and the H atoms bonded to C and O atoms are omitted. The atoms marked with an asterisk (*) or a hash (#) are at the symmetry positions $(1 + x, y, z)$ and $(-1 + x, y, z)$, respectively.

Table 4
Selected intermolecular hydrogen bonds (Å, °).

$D-H\cdots A$	$H\cdots A$	$D\cdots A$	$D-H\cdots A$
(1)			
N6—H6A$\cdots$O4^{i}	2.01	2.818 (4)	152
O1—H1Y$\cdots$O5^{ii}	1.75	2.688 (4)	172
O2—H2Y$\cdots$O3	1.70	2.635 (4)	176
O3—H3Y$\cdots$O1^{iii}	2.07	2.914 (4)	149
O4W—H4X$\cdots$O4^{iv}	2.06	2.880 (4)	145
O4W—H4X$\cdots$N5^{iv}	2.43	3.220 (5)	141
(3)			
N6—H6A$\cdots$O4^{v}	1.91	2.781 (3)	168
O21—H21A$\cdots$O2	2.04	2.846 (3)	167
O2—H21B$\cdots$O5^{vi}	1.88	2.711 (3)	175
(4)			
N6—H6A$\cdots$O4^{v}	1.92	2.790 (2)	169
O21—H21A$\cdots$O2	2.01	2.812 (2)	164
O2—H21B$\cdots$O5^{vi}	1.85	2.699 (2)	173
(5)			
N16—H16A$\cdots$O14^{iii}	2.00	2.845 (7)	161
N26—H26A$\cdots$O24^{vii}	2.04	2.873 (6)	158
O1—H1A$\cdots$O11^{i}	1.99	2.809 (6)	158
O1—H1B$\cdots$O22^{viii}	1.91	2.750 (5)	164
O4—H4B$\cdots$N15^{ix}	2.16	3.012 (6)	159
O4—H4B$\cdots$O14^{ix}	2.47	3.134 (4)	131
O6—H6B$\cdots$O24^{x}	2.32	3.160 (6)	147
O6—H6B$\cdots$N25^{x}	2.28	3.083 (8)	142
(6)			
N6—H6A$\cdots$O4^{xi}	2.03	2.841 (4)	153
N21—H21$\cdots$O23^{xii}	2.13	2.928 (4)	151
N22—H22$\cdots$N5^{xiii}	2.26	3.041 (4)	148
(7)			
N22—H22$\cdots$N5^{xiv}	2.27	3.077 (4)	152
(8)			
N16—H16A$\cdots$O14^{i}	2.13	2.997 (2)	170
N26—H26A$\cdots$O24^{xv}	2.20	3.073 (2)	175
N36—H36A$\cdots$O34^{xv}	2.03	2.830 (2)	150
N46—H46A$\cdots$O44^{i}	2.04	2.871 (2)	158
O1—H1A$\cdots$O422^{xv}	2.03	2.811 (2)	154
O7—H7A$\cdots$O45^{xvi}	1.93	2.723 (2)	155
O7—H7B$\cdots$O35^{xvii}	2.02	2.815 (2)	155
(9)			
N16—H16A$\cdots$O14^{v}	2.07	2.890 (5)	155
N26—H26A$\cdots$O24^{v}	2.07	2.875 (5)	152

Symmetry codes: (i) $1+x, y, z$; (ii) $x, -1+y, -1+z$; (iii) $x, 1+y, z$; (iv) $1+x, y, -1+z$; (v) $x, y, 1+z$; (vi) $\frac{3}{2}-x, -\frac{1}{2}+y, -z$; (vii) $x, -1+y, z$; (viii) $1+x, 1+y, z$; (ix) $1+x, 1+y, 1+z$; (x) $-1+x, -1+y, -1+z$; (xi) $-\frac{1}{2}+x, -\frac{1}{2}+y, z$; (xii) $\frac{1}{2}+x, -\frac{1}{2}+y, z$; (xiii) $\frac{3}{2}-x, \frac{5}{2}-y, -z$; (xiv) $\frac{1}{2}-x, \frac{1}{2}-y, -z$; (xv) $-1+x, y, z$; (xvi) $2-x, \frac{1}{2}+y, 2-z$; (xvii) $2-x, -\frac{1}{2}+y, 2-z$.

drate (Low, Arranz, Cobo, Fontecha, Godino, López et al., 2001). In each of (6) and (7) the cations lie on twofold rotation axes in the space group $C2/c$, and in each the cation is eight-coordinate: the coordination polyhedron in each case consists of two monodentate carboxylate units, two amidic O atoms and four water molecules. The tetrahydrate Sr salt is, in fact, almost isomorphous with the trihydrated Ca salt: in this trihydrate, each of the three water molecules is coordinated to Ca, but each is disordered over two sites related by the twofold rotation axis and thus having equal occupancy. Because of the fully correlated site occupancies at each indi-
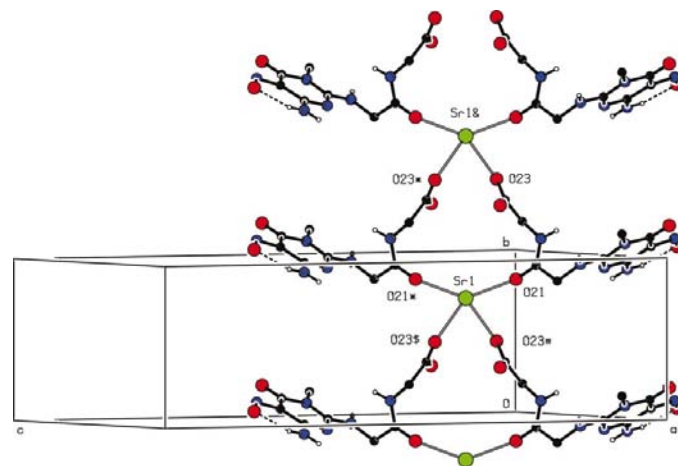
Figure 12
Part of the crystal structure of (6) showing the formation of a one-dimensional coordination polymer along [010]. For the sake of clarity, the water molecules and the H atoms bonded to C atoms are omitted. The atoms marked with an asterisk (*), a hash (#) or a dollar sign ($) are at the symmetry positions $(1-x, y, \frac{1}{2}-z)$, $(x, -1+y, z)$ and $(1-x, -1+y, \frac{1}{2}-z)$, respectively, and the Sr1& atom is at the position $(\frac{1}{2}, 1+y, 0.25)$.
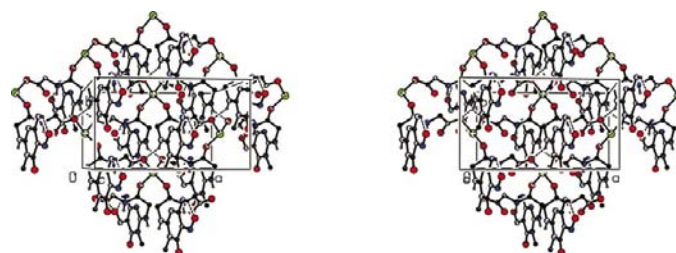
Figure 13
Stereoview of part of the crystal structure of (7) showing the formation of a two-dimensional coordination polymer as a deeply puckered (001) sheet. For the sake of clarity, the water molecules and the H atoms bonded to C atoms are omitted.
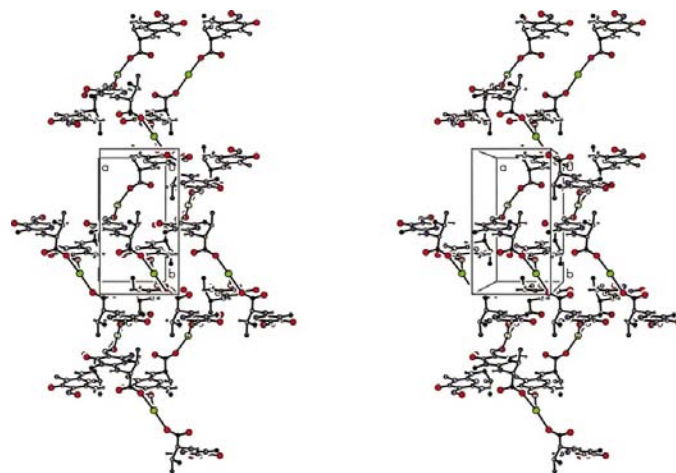
Figure 14
Stereoview of part of the crystal structure of (8) showing the formation of a (001) sheet of $R_8^4(44)$ rings, built from the type 1 cation and two anions only. For the sake of clarity, H atoms bonded to C atoms are omitted and only the major components of the disordered fragments are shown.

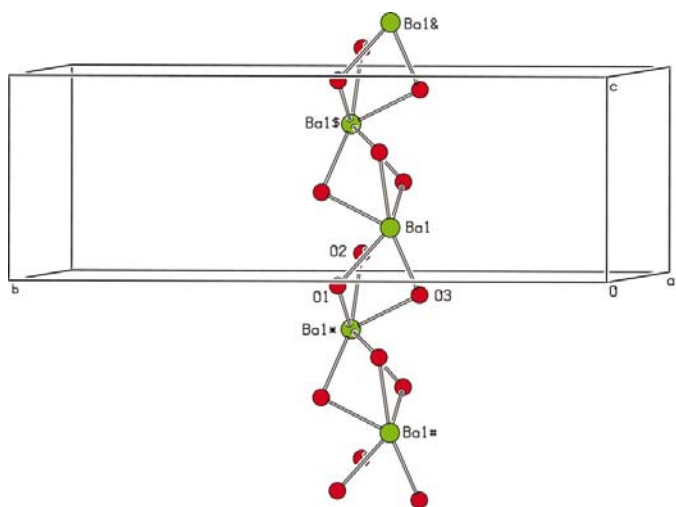vidual Ca ion, these ions are thus seven-coordinate with a geometry best described as distorted pentagonal bipyramidal.

Compound (8) crystallizes as a hexahydrate, but its constitution differs from those of all the other complexes in this series in that there are two distinct Ca cations, both lying in general positions, having entirely different coordination characteristics (Fig. 8). The first cation type, denoted Ca1, has eight coordination comprising two carboxylate groups from two different ligands, each bonded in monodentate mode, two nitroso O atoms from a further pair of anionic ligands, and four water molecules. The second cation type, denoted Ca2, has seven coordination, comprising two monodentate carboxylate groups, from a third pair of ligands, and five water molecules. There are in addition three more water molecules which are not directly coordinated to either of the cations. Hence, the appropriate formulation for the constitution of (8) is $[Ca(L^E)_2 \cdot (H_2O)_4] \cdot [Ca(L^E)_2 \cdot (H_2O)_5] \cdot 3H_2O$. As discussed

below (§3.3.3) the coordination polymers based on Ca1 and Ca2 are entirely different: Ca1 gives rise to a two-dimensional coordination polymer, while Ca2 forms a finite, zero-dimensional coordination complex.

The overall composition of the barium complex (9) (Fig. 9) is similar to that of complex (5), namely a heptahydrate. Again the Ba cation is ten-coordinate, but the composition of the coordination shell is different from that in (5). In (9) each cation is coordinated by seven water molecules, of which six are shared in two sets of three with two other cations; in addition, there are two monodentate carboxylate groups, compared with the one monodentate and one bidentate carboxylate in (5), and one nitroso O atom: nitroso coordination is absent from (5). The coordination characteristics of the two anions in (9) are therefore different as only one anion bridges pairs of cations. There are also three further water molecules linked to the rest of the structure by $O{-}H{\cdots}O$ hydrogen bonds.

Compounds (1), (3) and (8) provide examples of calcium(II) adopting six-, seven- and eight-coordination. For Ca^{2+} cations with these coordination numbers, Shannon & Prewitt (1970) have proposed ionic radii of 1.00, 1.07 and 1.12 Å, respectively. While the mean values of the Ca—O distances listed in Table 2 certainly increase with increasing coordination numbers, the mean distances involving the O atoms in the anions show a sharper rate of increase with coordination number, while the mean distances involving water molecules show a lesser increase than these radii would suggest. Compound (2) contains eight-coordinate Ba^{2+}, while compounds (5) and (9) both contain ten-coordinate Ba^{2+}: for such cations, Shannon and Prewitt's radii are 1.42 and 1.52 Å, respectively. Consistent with this, the mean value of the Ba—O distances in (2) is 2.777 Å, while the corresponding values for (5) and (9) are 2.873 and 2.888 Å, respectively.
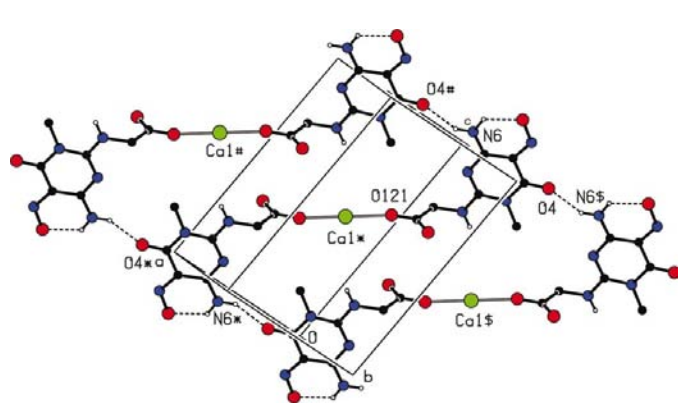

Figure 15
Stereoview of part of the crystal structure of (9) showing the formation of a 4_3 helical chain along $(\frac{1}{2}, \frac{1}{2}, z)$ built from cations and type 2 anions only. For the sake of clarity H atoms bonded to C atoms are omitted and only the major components of the disordered fragments are shown.

Figure 16
Part of the crystal structure of (9) showing the formation of a 2_1 helical chain along $(1, \frac{1}{2}, z)$ built from only cations and water molecules. The atoms marked with an asterisk (*), a hash (#), a dollar sign ($) or an ampersand (&) are at the symmetry positions $(2-x, 1-y, -\frac{1}{2}+z)$, $(x, y, -1+z)$, $(2-x, 1-y, \frac{1}{2}+z)$ and $(x, y, 1+z)$, respectively.

Figure 17
Part of the crystal structure of (1) showing the formation of a hydrogen-bonded molecular ladder along [100] formed by cations and anions alone. For the sake of clarity, the water molecules and the H atoms bonded to C atoms are omitted. The O and N atoms marked with an asterisk (*), a hash (#) or a dollar sign ($) are at the symmetry positions $(1-x, 1-y, 1-z)$, $(1+x, y, z)$ and $(-1+x, y, z)$, respectively, and atoms Ca1*, Ca1# and Ca1$ are at the positions $(\frac{1}{2}, \frac{1}{2}, \frac{1}{2})$, $(\frac{3}{2}, \frac{1}{2}, \frac{1}{2})$ and $(-\frac{1}{2}, \frac{1}{2}, \frac{1}{2})$, respectively.

3.2. Ligand dimensions and conformations

The pyrimidinone rings in (1)–(9) are all essentially planar and both the amino and the nitrosyl substituents are coplanar with the ring: only the N-substituent side chains deviate from this plane. The coplanarity of the amino groups with the pyrimidinone ring permits electronic delocalization between the various N atoms, but effectively precludes these atoms from acting as hydrogen-bond acceptors. In each compound the nitrosyl group is oriented *trans* to C4, so that its oxygen O5 is ideally placed for the formation of an intramolecular N—H$\cdots$O hydrogen bond in an $S(6)$ motif (Bernstein *et al.*, 1995).

Several of the bond lengths in (1)–(9) have unusual values. First, in the C-nitroso group the C—N and N—O bond distances are similar (Table 3): in simple neutral compounds where there is no possibility of significant electronic delocalization these distances normally differ by at least 0.20 Å (Talberg, 1977; Schlemper *et al.*, 1986) and the NO distance rarely exceeds 1.25 Å (Davis *et al.*, 1965; Bauer & Andreassen, 1972; Talberg, 1977; Schlemper *et al.*, 1986). On the other hand, the C—N and N—O distances in (1)–(9) are typical of those observed in oximate anions $[RR'C=N-O]^-$ (Raston *et al.*, 1978; Domasevitch, Gerasimchuk *et al.*, 1996; Domase-

vitch, Mokhir *et al.*, 1996; Domasevitch *et al.*, 1997, 1998). Secondly, the C5—C6 bond length in each of (1)–(9) is more typical of a single bond between two three-connected C atoms [mean value 1.460 Å (Allen *et al.*, 1987)] than of a double bond between two such atoms [mean value for C-substituted bonds 1.331 Å; typical values in N heterocycles lie in the range 1.36–1.38 Å]. Thirdly, the C—N bonds denoted *a*, *f*, *g* and *h* in Table 3 are all rather similar in length, such that it is not possible to distinguish between single and double bonds here. These geometric parameters taken together indicate that the conventional representation *A* is a less appropriate representation of the molecular and electronic structure in this series than the alternative, charge-separated form *B*.
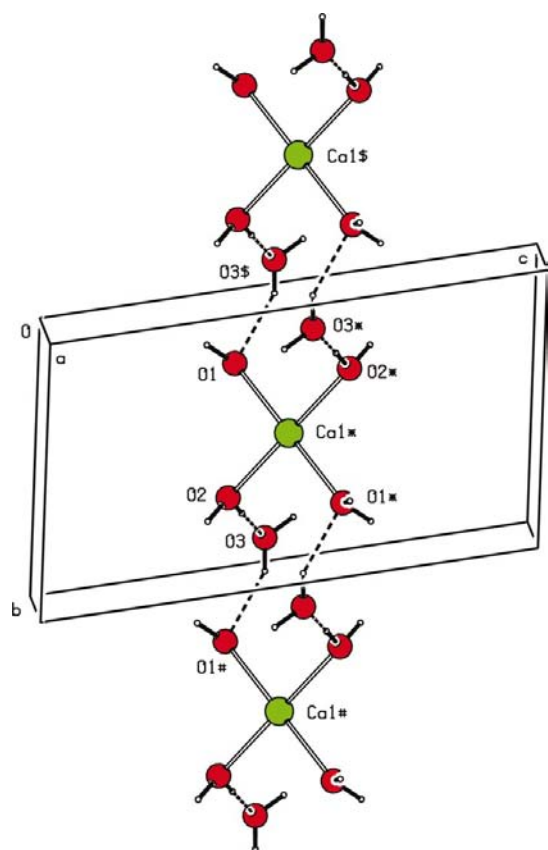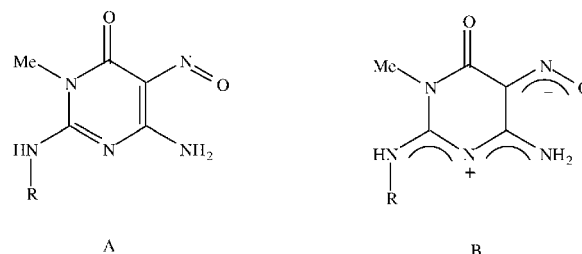

3.3. Coordination polymers

3.3.1. A zero-dimensional coordination polymer, (1). As noted above (§3.1) the calcium cation in (1) is coordinated only by two monodentate anions and by four water molecules (Fig. 1). Thus, no coordination polymer is formed here, and the supramolecular aggregation depends solely on hydrogen bonding.
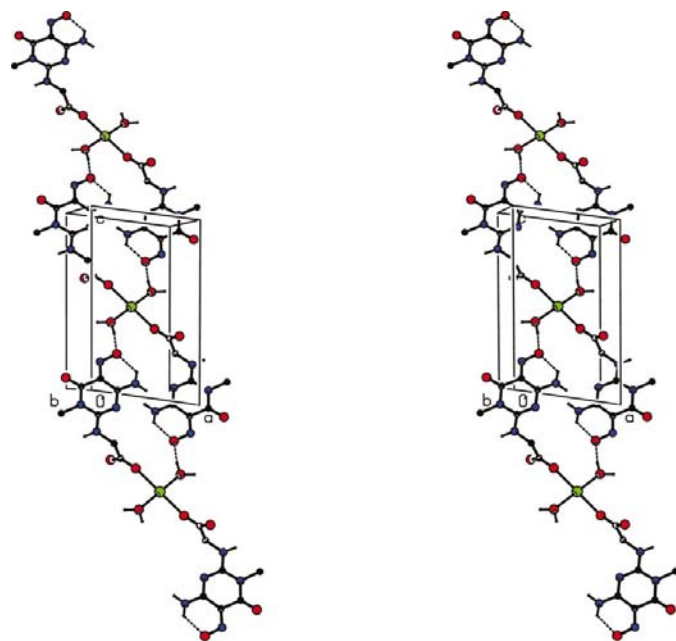

Figure 18
Part of the crystal structure of (1), showing the formation of a chain of spiro-fused rings along [010] built from cations and water molecules only. The O atoms marked with an asterisk (*), a hash (#) or a dollar sign ($) are at the symmetry positions $(1-x, 1-y, 1-z)$, $(x, 1+y, z)$ and $(x, -1+y, z)$, respectively, and atoms Ca1*, Ca1# and Ca1$ are at the positions $(\frac{1}{2}, \frac{1}{2}, \frac{1}{2})$, $(\frac{1}{2}, \frac{3}{2}, \frac{1}{2})$ and $(\frac{1}{2}, -\frac{1}{2}, \frac{1}{2})$, respectively.

Figure 19
Stereoview of part of the crystal structure of (1) showing the formation of a chain of spiro-fused rings along [110]. For the sake of clarity, the water molecules not involved in the motif shown and H atoms bonded to C atoms are omitted.

3.3.2. One-dimensional coordination polymers. Compound (2): This compound is isostructural with the strontium analogue (Glidewell *et al.*, 2002): the anions of type 2 bridge adjacent pairs of cations, producing a one-dimensional coordination polymer in the form of a simple chain generated by a 2_1 screw axis in the space group $P2_1/c$, while the type 1 anions are pendent from this chain.
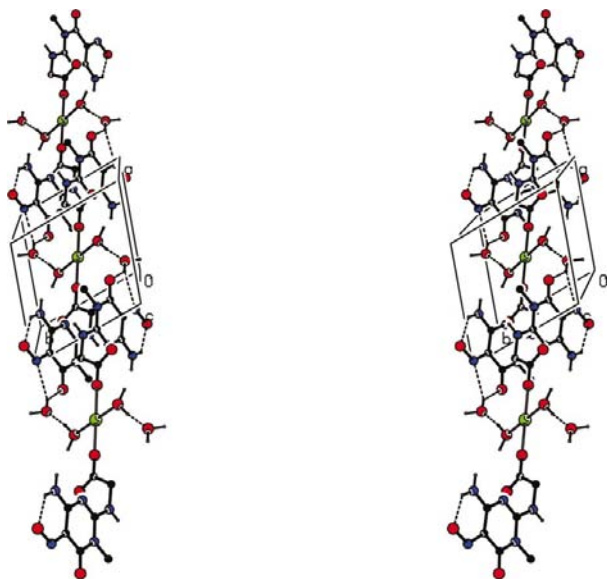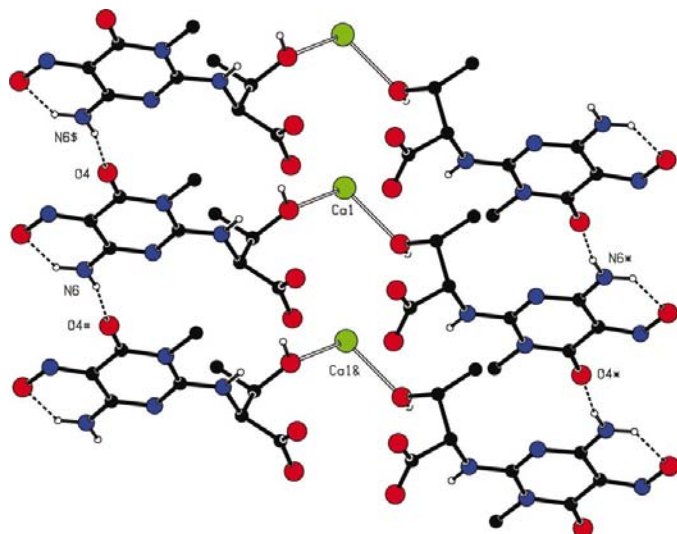

Figure 20
Stereoview of part of the crystal structure of (1) showing the formation of a chain of spiro-fused rings along [$10\bar{1}$]. For the sake of clarity, the water molecules not involved in the motif shown and H atoms bonded to C atoms are omitted.

Figure 21
Part of the crystal structure of (3) showing the formation of a hydrogen-bonded molecular ladder along [001]. For the sake of clarity, the water molecules, the H atoms bonded to C atoms and the unit-cell box are all omitted. The O and N atoms marked with an asterisk (*), a hash (#) or a dollar sign ($) are at the symmetry positions $(2 - x, y, 1 - z)$, $(x, y, 1 + z)$ and $(x, y, -1 + z)$, respectively, and the Ca1& atom is at the position $(1, 1 + y, \frac{1}{2})$.

Compounds (3) and (4): These compounds are isostructural, and hence only (3) will be discussed in any detail. In (3) the calcium cation lies on a twofold rotation axis in the space group $C2$, chosen as that along $(1, y, \frac{1}{2})$, and the anion acts as a bridging ligand between pairs of calcium ions. The reference Ca centre is ligated by the hydroxyl O21 atoms of the anions at (x, y, z) and $(2 - x, y, 1 - z)$, while the carboxyl groups in the two anions coordinate in bidentate fashion to the Ca at $(1, 1 + y, \frac{1}{2})$. In this way a coordination polymer is generated in the form of a chain of spiro-fused rings, running parallel to the [010] direction (Fig. 10). In both (3) and (4) the metal coordination is completed by a pair of symmetry-related water molecules, containing O1 (Figs. 3 and 4), and in both compounds the $M-O$ distances (Table 2) follow the same order: $M-O1 < M-O22 < M-O21 < M-O23$, although the difference between the two $M-O$ distances involving the bidentate carboxylate group is significantly less for $M = Sr$ than for Ca.

Compound (5): While the coordination polymer formed by (5) (Fig. 5) is one-dimensional, as in (3) and (4), with each anionic ligand bridging a pair of metal cations, there are two independent anions in (5) whose ligating properties are different. There is thus no internal symmetry in the polymer chain. While in the type 1 anionic ligand, containing atoms O11, O12 and O13, the carboxylate unit acts as a bidentate ligand, in the type 2 anion (containing atoms O21, O22 and O23) the carboxylate acts as a monodentate ligand. Nonetheless, the coordination polymer again consists of a chain of spiro-fused rings (Fig. 11), in this case running parallel to the [100] direction. In addition to the five ligating O atoms from the two anions, the Ba cation is also coordinated by four of the
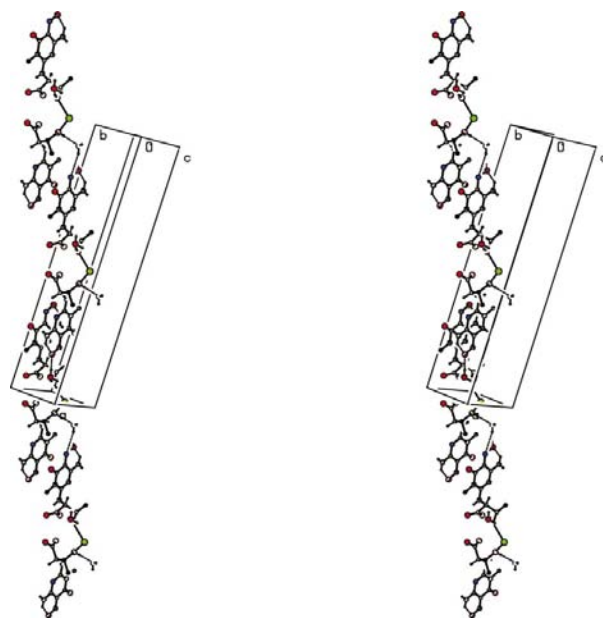

Figure 22
Stereoview of part of the crystal structure of (3) showing the formation of a hydrogen-bonded molecular ladder along [102]. For the sake of clarity, the water molecules not involved in the ladder depicted and the H atoms bonded to the C atoms are omitted.

seven water molecules (those containing O1–O4), so giving nine-coordination. It may be noted here that the difference between the two $M{-}O$ distances involving the bidentate carboxylate unit in (5) is less than in either of (3) and (4), (Table 2).

Compound (6): In (6) (Fig. 6), the Sr cation lies on a twofold rotation axis in the space group $C2/c$, chosen as that along $(\frac{1}{2}, y, \frac{1}{4})$. The anionic ligand bridges two Sr cations, which are ligated by amidic O21 of the anion at (x, y, z) and carboxylate O23 of the anion at $(x, -1 + y, z)$. In this manner, a one-dimensional coordination polymer is generated in which the cations and anions form a chain of spiro-fused $R_4^2(14)$ (Starbuck *et al.*, 1999) rings (Fig. 12). Four chains of this type run through each unit cell, along the axes $(\frac{1}{2}, y, \frac{1}{4})$, $(\frac{1}{2}, -y, \frac{3}{4})$, $(0, y, \frac{1}{4})$ and $(0, -y, \frac{3}{4})$.

3.3.3. A two-dimensional coordination polymer, (7).

In (7) (Fig. 7) the cation again lies on the twofold rotation axis along $(\frac{1}{2}, y, \frac{1}{4})$ in $C2/c$, with a similar set of ligating atoms to those in (6). However, the carboxylate atoms O23 coordinated to the reference Ba are those in the anions at $(\frac{1}{2} + x, \frac{1}{2} + y, z)$ and $(\frac{1}{2} - x, \frac{1}{2} + y, \frac{1}{2} - z)$. The amidic O21 atoms in these two anions are coordinated to cations at $(1, \frac{1}{2} + y, \frac{1}{4})$ and $(0, \frac{1}{2} + y, \frac{1}{4})$, respectively. The carboxylate O23 atoms in the anions at (x, y, z) and $(1 - x, y, \frac{1}{2} - z)$ (whose amidic O21 atoms are bonded to the reference Ba) are coordinated to Ba ions at $(0, -\frac{1}{2} + y, \frac{1}{4})$ and $(1, -\frac{1}{2} + y, \frac{1}{4})$. In this manner, each anion is coordinated to two different Ba cations, while each Ba is bonded to four different anions, thus producing a two-dimensional coordination polymer. The polymer forms deeply puckered (001) sheets, in the form of a (4,4) net (Batten & Robson, 1998) built from a single type of $R_8^4(28)$ ring (Fig. 13). Two sheets of this type pass through each unit cell: in one sheet all of the Ba have $z = \frac{1}{4}$ and in the other all of the Ba have $z = \frac{3}{4}$.
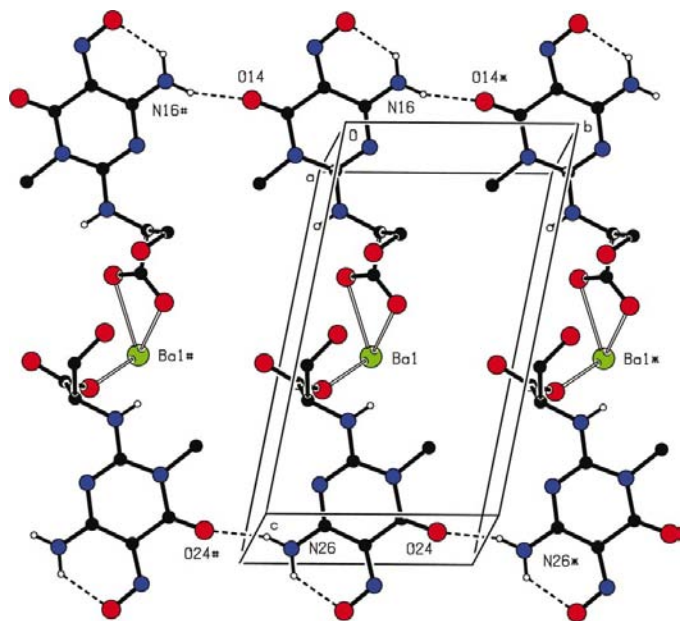
3.3.4. A coordination polymer with mixed dimensionality, (8).

The coordination polymer based on the type 1 cation Ca1 in (8) takes the form of a (4,4) net (Batten & Robson, 1998). The type 1 and type 2 anions (containing N11 *etc.* and N21 *etc.*, respectively) at (x, y, z) are coordinated to Ca1 at (x, y, z) in monodentate fashion *via* their carboxylate O atoms O121 and O221. In the same pair of anions, the nitroso O atoms O15 and O25 are coordinated respectively to the Ca1 cations at $(-x, \frac{1}{2} + y, 1 - z)$ and $(1 - x, -\frac{1}{2} + y, 1 - z)$, so forming a chain along
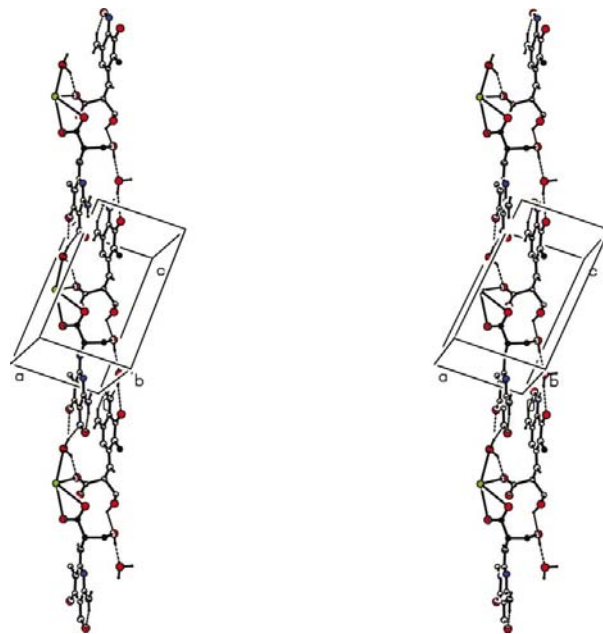

Figure 24
Stereoview of part of the crystal structure of (5) showing the formation of a hydrogen-bonded molecular ladder along [111]. For the sake of clarity, the water molecules not involved in the ladder depicted and the H atoms bonded to the C atoms are omitted.
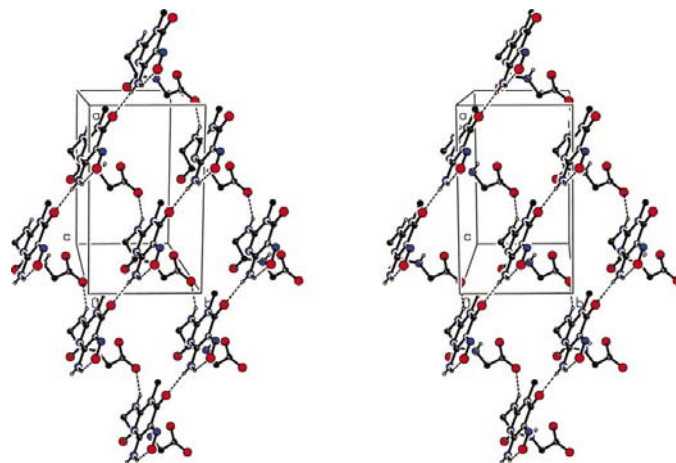

Figure 23
Part of the crystal structure of (5) showing the formation of a hydrogen-bonded molecular ladder along [010]. For the sake of clarity, the water molecules and the H atoms bonded to C and O atoms are omitted. The atoms marked with an asterisk (*) or a hash (#) are at the symmetry positions $(x, 1 + y, z)$ and $(x, -1 + y, z)$, respectively.

Figure 25
Stereoview of part of the crystal structure of (6) showing the linking of the coordination polymer chains into hydrogen-bonded (001) sheets of $R_4^4(36)$ rings. For the sake of clarity, the water molecules and the H atoms bonded to C atoms are omitted.

[1$\bar{1}$0]. At the same time, the reference Ca1 cation at (x, y, z) is also coordinated by nitroso O15 and O25 atoms in the anions at $(-x, -\frac{1}{2} + y, 1 - z)$ and $(1 - x, \frac{1}{2} + y, 1 - z)$, respectively, thus forming a similar chain along [110], which is related to the [1$\bar{1}$0] chain by the action of the 2_1 screw axes at $z = 0.5$. The combination of [110] and [1$\bar{1}$0] chains generates a (001) sheet built from a single type of $R_4^8(44)$ ring (Starbuck *et al.*, 1999), with the cations forming the nodes of the (4,4) net (Fig. 14). Just one sheet of this type passes through each unit cell, occupying the domain $0.28 < z < 0.72$, that is to say, somewhat less than one half of the available volume.

By contrast, the coordination of the type 2 cation Ca2 leads only to a monomeric coordination complex $[Ca(L^E)_2(H_2O)_5]$ (*cf.* Fig. 8*b*): this complex lies in the domain $0.75 < z < 1.10$ and a symmetry-related complex lies in the domain $-0.10 < z < 0.25$. There is thus no overlap between the monomeric complexes containing Ca2 and the sheets containing Ca1; the two coordination types are, however, linked by an extensive series of hydrogen bonds (see §3.4.6).

3.3.5. A three-dimensional coordination polymer, (9). The coordination polymer in (9) is three-dimensional and its construction can most readily be analysed in terms of two distinct one-dimensional substructures. These involve, respectively, the cation and one of the anions, and the cation and three of the water molecules. In the first coordination polymer motif, nitroso O25 in the type 2 anion (containing N21, N22 *etc.*) at (x, y, z) is coordinated to the Ba cation at $(1 - y, x, -\frac{1}{4} + z)$, while O25 at $(1 - y, x, -\frac{1}{4} + z)$ is in turn coordinated to the cation at $(1 - x, 1 - y, -\frac{1}{2} + z)$: propagation of this interaction thus generates a $C(11)$ (Starbuck *et al.*,
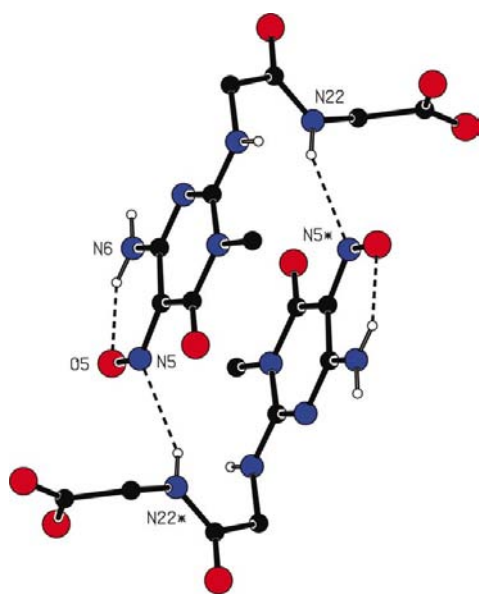
1999) helical chain running parallel to the [001] direction and generated by the 4_3 screw axis along $(\frac{1}{2}, \frac{1}{2}, z)$ (Fig. 15). It is intersting to note that the disordered methionine units lie within this helical chain. A single chain of this type passes through each unit cell. Since these amino acid units carry no hydrogen-bonding functionality, there is effectively no tethering of these distal ends and the extensive disorder is probably associated with the terminal ends of these: indeed, it is quite likely that the methionine units are rather mobile within the core of the helical polymer.

In the second coordination polymer motif, the water molecules containing O1, O2 and O3 at (x, y, z) are coordinated to the Ba cation at $(2 - x, 1 - y, -\frac{1}{2} + z)$, while the corresponding water molecules at $(2 - x, 1 - y, -\frac{1}{2} + z)$ are in turn coordinated to the cation at $(x, y, -1 + z)$. Hence a chain of cation and water molecules is generated by the 2_1 screw axis along $(1, \frac{1}{2}, z)$ (Fig. 16), with equivalent chains along $(0, \frac{1}{2}, z)$, $(\frac{1}{2}, 0, z)$ and $(\frac{1}{2}, 1, z)$. The cations at (x, y, z) and at $(2 - x, 1 - y, -\frac{1}{2} + z)$ lie respectively in the 4_3 helices along $(\frac{1}{2}, \frac{1}{2}, z)$ and $(\frac{3}{2}, \frac{1}{2}, z)$, so that the combined effect of the 2_1 helices is to link together all of the 4_3 helices into a single continuous framework.

3.4. Hydrogen bonding

The polarized molecular-electronic structures of the anionic ligands (§3.2) lead to the development of charge-assisted hydrogen bonding (Gilli *et al.*, 1994). Extensive hydrogen bonding is present in all of the structures, and in Table 4 are listed only those hydrogen bonds which form part of the
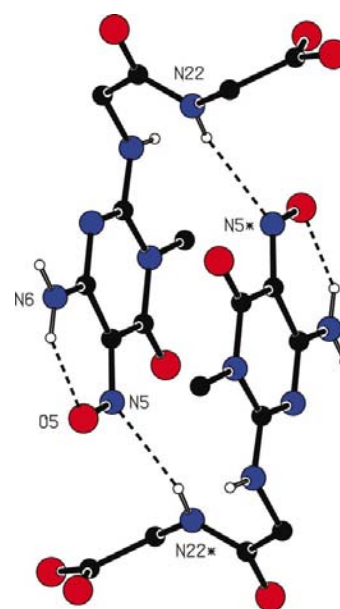

Figure 26
Part of the crystal structure of (6) showing the formation by the anionic ligands of a hydrogen-bonded $R_2^2(20)$ ring which links the (001) bilayers. For the sake of clarity, the H atoms bonded to C atoms and the unit-cell box are omitted. The atoms marked with an asterisk (*) are at the symmetry position $(\frac{3}{2} - x, \frac{5}{2} - y, -z)$.

Figure 27
Part of the crystal structure of (7) showing the formation by the anionic ligands of a hydrogen-bonded $R_2^2(20)$ ring which links the (001) sheets. For the sake of clarity, the H atoms bonded to C atoms and the unit-cell box are omitted. The atoms marked with an asterisk (*) are at the symmetry position $(\frac{1}{2} - x, \frac{1}{2} - y, -z)$.

discussions below: full listings are available in the CIF, which forms part of the supplementary material.

3.4.1. Compound (1). Although the coordination aggregate in (1) is finite and thus effectively zero-dimensional (Fig. 1), the extensive hydrogen bonding links these units into a continuous three-dimensional framework. Each anionic ligand has two N—H bonds available for inter-aggregate hydrogen bonding, while there is a total of 12 O—H bonds per aggregate available for this purpose. There are hydrogen-bonded chains running along the [100], [010], [110] and [10$\bar{1}$] directions, which combine to build the framework.

Amino N6 in the anion at (x, y, z) is part of the aggregate centred at $(\frac{1}{2}, \frac{1}{2}, \frac{1}{2})$ and it acts as a hydrogen-bond donor, via H6A, to amidic O4 at $(1 + x, y, z)$, part of the aggregate centred at $(\frac{3}{2}, \frac{1}{2}, \frac{1}{2})$. Propagation of this hydrogen bond by inversion and translation then produces a molecular ladder running parallel to the [100] direction (Fig. 17), in which the uprights are a pair of antiparallel $C(6)$ chains with 36-membered rings between the rungs formed from the Ca-amino acid fragments. The cations and three of the four independent water molecules give rise to a chain along [010] without any participation of the anions. Water O2 at (x, y, z) is coordinated to the cation at $(\frac{1}{2}, \frac{1}{2}, \frac{1}{2})$, which acts as a donor to water O3, also at (x, y, z), while O3 at (x, y, z) acts as a donor to water O1 at $(x, 1 + y, z)$, which is coordinated to the cation at $(\frac{1}{2}, \frac{3}{2}, \frac{1}{2})$. In this manner a chain of spiro-fused 12-membered rings is formed (Fig. 18). The water O1 at (x, y, z) in turn acts as a hydrogen-bond donor, via H1Y, to the nitroso O5 in the anion at $(x, -1 + y, -1 + z)$, which forms part of the aggregate

centred at $(\frac{1}{2}, -\frac{1}{2}, -\frac{1}{2})$. Propagation of the hydrogen bond leads to the formation of a chain of spiro-fused rings running parallel to the [110] direction (Fig. 19). Finally, water O4W at (x, y, z) acts as a donor to both N5 and O4 in the anion at $(1 + x, y, -1 + z)$, a component of the aggregate centred at $(\frac{3}{2}, \frac{1}{2}, -\frac{1}{2})$, in an effectively planar three-centre O—H$\cdots$(N,O) hydrogen bond, thus forming another chain of spiro-fused rings, this time running parallel to [10$\bar{1}$] (Fig. 20).

3.4.2. Compound (2). The linking of the coordination-polymer chains into a three-dimensional framework is exactly the same as in the isostructural Sr complex (Glidewell *et al.*, 2002). The patterns of the hydrogen bonds in the two complexes are identical and their dimensions are almost the same.

3.4.3. Compounds (3) and (4). Again, it is necessary only to discuss one member of this isomorphous pair, (3). In this structure, an extensive series of hydrogen bonds, involving both the anionic ligands and the water molecules, links the coordination-polymer chains into a single continuous framework, and we discuss only the minimal set of such interactions required to demonstrate the three-dimensional nature of the structure.

The ionic components alone form molecular ladders running parallel to the [001] direction (Fig. 21): the anion at (x, y, z) lies in the polymer chain along $(1, y, \frac{1}{2})$, and the amino N6 at (x, y, z) acts as a hydrogen-bond donor, via H6A, to the amido O4 in the anion at $(x, y, 1 + z)$, which forms part of the polymer chain along $(1, y, \frac{3}{2})$. Within the ladder the uprights are formed by two antiparallel $C(6)$ chains built from N—H$\cdots$O hydrogen bonds, while the rungs consist of the Ca ions and pairs of threonine side chains. Between the rungs are puckered 36-membered rings. Propagation of the N—H$\cdots$O hydrogen bond via the twofold rotation axes links together the polymer chains into (100) sheets.

A second molecular ladder, running parallel to the [102] direction, incorporates the water molecule containing O2. The
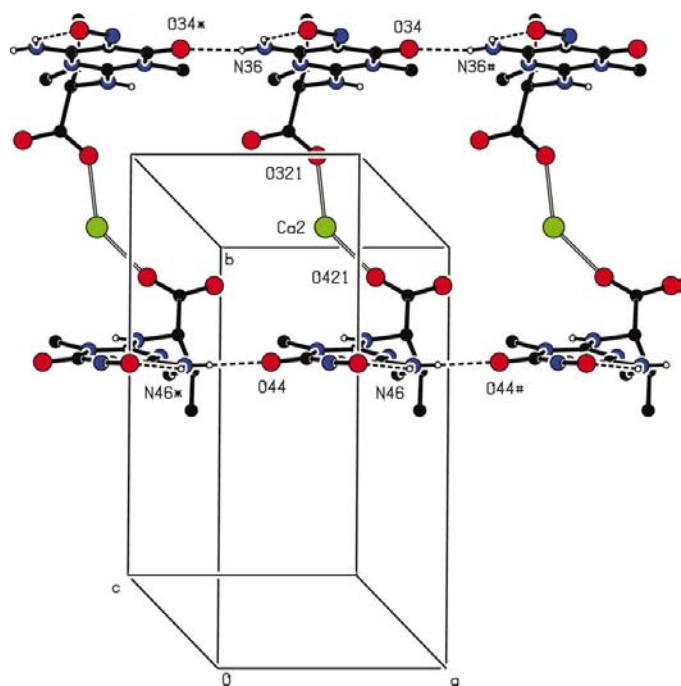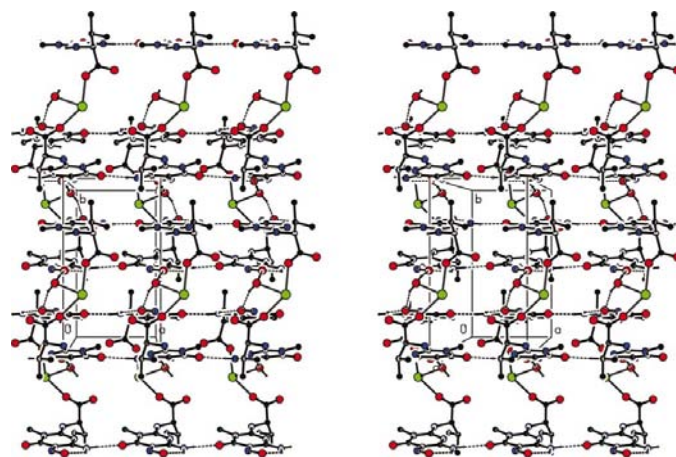

Figure 28
Part of the crystal structure of (8) showing the formation of a hydrogen-bonded molecular ladder along [100] formed by Ca2 and its coordinated anions. For the sake of clarity, H atoms bonded to C atoms are omitted. The atoms marked with an asterisk (*) or a hash (#) are at the symmetry positions $(-1 + x, y, z)$ and $(1 + x, y, z)$, respectively.

Figure 29
Stereoview of part of the crystal structure of (8) showing the linking of the [100] ladders into a (001) sheet by water molecules. For the sake of clarity, H atoms bonded to C atoms are omitted and only the major components of the disordered fragments are shown.

O21 atom in the anion at (x, y, z) lies in the polymer chain along $(1, y, \frac{1}{2})$, and it acts as a donor to water O2, also at (x, y, z): this water molecule acts as a hydrogen-bond donor, *via* H21*B*, to nitroso O5 in the anion at $(\frac{3}{2} - x, -\frac{1}{2} + y, -z)$, which forms part of the polymer chain along $(\frac{1}{2}, y, -\frac{1}{2})$. Propagation of this O—H$\cdots$O hydrogen bond, by the twofold rotation axes, generates the [102] ladder (Fig. 22) which in turn links the polymer chain into a sheet parallel to (201). The combination of the (100) and (201) sheets is sufficient to generate the three-dimensional framework.

3.4.4. Compound (5). Although all the components of (5) lie in general positions with two independent anions and although the space group is $P\bar{1}$, compared with $C2$ in (3) and (4), nonetheless, a number of the hydrogen-bonding motifs in (5) are somewhat similar to those in (3) and (4). The amino N16 and N26 in the anions at (x, y, z) act as hydrogen-bond donors, *via* H16*A* and H26*A*, respectively, to amidic O14 at $(x, 1 + y, z)$ and O24 at $(x, -1 + y, z)$, thus generating a molecular ladder running parallel to the [010] direction (Fig. 23). This ladder is very similar in construction to the [001] ladder in (3) and (4) (Fig. 21) and it links the [100] polymer chains into a (001) sheet.

The very extensive array of hydrogen bonds, mostly of the O—H$\cdots$O type, involving the water molecules (Table 4), generates further chain motifs, running parallel to the [100], [110] and [111] directions, which together with the [010] ladder link the polymer chains into a single, tightly bound three-dimensional framework. Thus, for example, coordinated water O4 at (x, y, z), acts as a donor, *via* H4*B*, to both O14 and N15 in the type 1 anion at $(1 + x, 1 + y, 1 + z)$ in a planar three-centre O—H$\cdots$(N,O) hydrogen bond, while O6 at (x, y, z) likewise acts as a donor, *via* H6*B*, to both O24 and N25 in the type 2 anion at $(-1 + x, -1 + y, -1 + z)$, thus forming a ladder running parallel to the [111] direction (Fig. 24).

3.4.5. Compound (6). The one-dimensional coordination-polymer chains along [010] in (6) are linked by hydrogen bonds into a three-dimensional framework of some complexity. The analysis and the description of the formation of this framework are both markedly simplified by the observation that it can be described in terms of the ionic components only. Although the hydrogen bonds formed by the water molecules undoubtedly reinforce the framework, their presence is not essential to demonstrate its three-dimensional nature.

The amino N21 atom in the anion at (x, y, z) acts as a hydrogen-bond donor to carboxylate O23 in the anion at $(\frac{1}{2} + x, -\frac{1}{2} + y, z)$, thus producing a $C(8)$ chain running parallel to the [1$\bar{1}$0] direction and generated by the C-centring operation of the space group $C2/c$. Similarly, amino N6 in the anion at (x, y, z) acts as a hydrogen-bond donor, *via* H6*A*, to amido O4 in the anion at $(-\frac{1}{2} + x, -\frac{1}{2} + y, z)$, thus producing a $C(6)$ chain along [110], again generated by the C-centring operation. The combination of these two chain motifs produces a (001) sheet in the form of a (4,4) net built from a single type of $R_4^4(36)$ ring (Fig. 25). There are four such sheets passing through each unit and they are linked in pairs by the cations into two bilayers, one lying in the domain $-0.09 < z <$ 0.59, where the hydrogen-bonded sheets are linked by the cations at $z = 0.25$, and the other in the domain $0.41 < z < 1.09$, where the sheets are linked by the cations at $z = 0.75$.

The bilayers are linked together by a third hydrogen bond, again involving only the anion. The amido N22 atom in the anion at (x, y, z), which lies in the bilayer generated by the twofold axes at $z = \frac{1}{4}$, acts as a hydrogen-bond donor to the nitroso N5 in the anion at $(\frac{3}{2} - x, \frac{5}{2} - y, -z)$, which lies in the bilayer generated by the twofold axes at $z = -0.25$. The resulting $R_2^2(20)$ ring (Fig. 26), when propagated by the space-group operators, serves to link each bilayer to its two immediate neighbours and hence to link all the bilayers into a single continuum. The two pyrimidine rings in this centro-symmetric motif are parallel with an interplanar spacing of 3.320 (2) Å and a centroid separation of 3.730 (2) Å, corresponding to a centroid offset of 1.700 (2) Å, indicative of a weak and possibly adventitious aromatic $\pi\cdots\pi$ stacking interaction.

3.4.6. Compound (7). As in (6), there is an extensive series of hydrogen bonds in (7). However the linking of the (001) coordination-polymer sheets is most simply demonstrated in terms of a single N—H$\cdots$N hydrogen bond. The amino N22 in the anion at (x, y, z) lies in the reference sheet having a Ba cation at $z = 0.25$: this N22 acts as a hydrogen-bond donor to
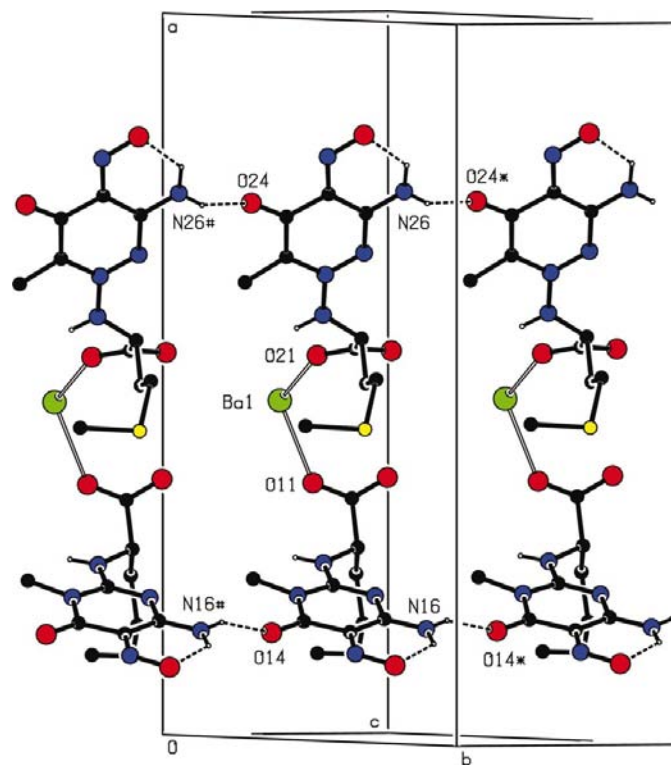

Figure 30
Part of the crystal structure of (9) showing the formation of a hydrogen-bonded molecular ladder along [001] formed by the cation and the anions only. For the sake of clarity, H atoms bonded to C atoms are omitted and only the major components of the disordered fragments are shown. The atoms marked with an asterisk (*) or a hash (#) are at the symmetry positions $(x, y, 1 + z)$ and $(x, y, -1 + z)$, respectively.

nitroso N5 in the anion at $(\frac{1}{2} - x, \frac{1}{2} - y, -z)$, which lies in the polymer sheet having Ba cations at $z = -\frac{1}{4}$. Propagation by the space group of the resulting $R_2^2(20)$ motif (Fig. 27) links each polymer sheet to the two neighbouring sheets and hence all the sheets are linked into a single framework. As in (6), this $R_2^2(20)$ ring appears to be weakly reinforced by an aromatic $\pi \cdots \pi$ stacking interaction: the interplanar separation of the two pyrimidine rings is 3.316 (2) Å, with a centroid separation of 3.794 (2) Å and a centroid offset of 1.843 (2) Å. It is striking that, despite the very different coordination-polymer substructures in (6) and (7), the same $R_2^2(20)$ motif is present in the hydrogen bonding of both structures.

3.4.7. Compound (8). The asymmetric unit of (8) contains 12 independent water molecules and four independent anions; the hydrogen bonding is therefore very extensive and of some considerable complexity. However, it is possible to demonstrate the three-dimensional framework structure of (8), into which are linked both the coordination monomer based upon Ca2 and the coordination polymer based upon Ca1, in terms of no more than five intermolecular hydrogen bonds out of the 30 or so available. The framework formation is conveniently analysed and described in terms firstly of the formation of molecular ladders generated by the Ca2 monomer and then in terms of the role of these ladders in linking the Ca1 and Ca2 moieties together.

In the anions of types 3 and 4, coordinated to Ca2 at (x, y, z), the amino N36 and N46 atoms act as hydrogen-bond donors, *via* H36*A* and H46*A*, respectively, to O35 at $(-1 + x, y, z)$ and to O44 at $(1 + x, y, z)$, thus generating by translation a ladder running parallel to the [100] direction. (Fig. 28). It may be noted here that within the coordination-polymer sheet based upon Ca1 it is possible to identify a molecular ladder, entirely analogous to that formed by Ca2 and its coordinated anions. In the [100] ladder (Fig. 28) the Ca2 cations lie along the line $(x, 0.87, 0.82)$ and in ladders related to it by the 2_1 screw axis the Ca2 cations lie along the lines $(x, 0.37, 1.18)$, $(x, 1.37, 1.18)$ and so on. The water molecule containing O7 links all the ladders whose Ca2 cations lie in the domain $0.82 < z < 1.18$ into a second type of (001) sheet. The water molecule containing O7 at (x, y, z) is directly coordinated to Ca2 at (x, y, z) and it acts as a hydrogen bond donor, *via* H7*A* and H7*B*, respectively to O45 in the type 4 anion at $(2 - x, \frac{1}{2} + y, 2 - z)$ and to O35 in the type 3 amino at $(2 - x, -\frac{1}{2} + y, 2 - z)$: these two anions lie in the ladders along $(x, 1.37, 1.18)$ and $(x, 0.37, 1.18)$ and propagation of these hydrogen bonds by translation generates a (001) sheet whose cations and anions occupy the domain $0.75 < z < 1.25$ (Fig. 29). In this manner a millefeuille structure is formed with alternating layers based upon Ca1 and Ca2 cations and their ligands.

One further hydrogen bond suffices to link the various layers into a continuum. The water molecule containing O1 is directly coordinated to Ca1 and this water at (x, y, z) lies in the $0.28 < z < 0.72$ layer: it acts as a hydrogen-bond donor, *via* H1*A*, to carboxyl O422 in the type 4 amino at $(-1 + x, y, z)$, which itself lies in the $0.75 < z < 1.25$ layer. Propagation of this hydrogen bond by the twofold screw axes serves to link each layer to its two neighbouring layers, thus forming a single framework.

3.4.8. Compound (9). Although the coordination polymer in (9) is three-dimensional, the resulting framework gains some reinforcement from the formation of a hydrogen-bonded molecular ladder. The amino N16 and N26 atoms in the two anions at (x, y, z) act as hydrogen-bond donors, *via* H16*A* and H26*A*, respectively, to O14 and O24 in the corresponding anions at $(x, y, 1 + z)$, thus generating by translation along [001] the same type of molecular ladder (Fig. 30), as observed in (1), (3). (4), (5) and (8).

4. Concluding comments

The title anions readily form hydrated neutral complexes with a range of M^{2+} cations, particularly Ca^{2+}, Sr^{2+} and Ba^{2+}, and the products exhibit a wide range of structural motifs, both in terms of the metal–ligand coordination and in terms of the hydrogen bonding. The dimensions of the nitrosopyrimidine rings all provide evidence for strong polarization of the electronic structures, as found earlier (Low *et al.*, 2000) for a series of related dihydropyrimidinones. Although the intramolecular distances are unusual in comparison with those in simple nitroso-arenes and in analogous pyrimidines carrying no nitroso substituent, a simple polarization model is consistent with all the present observations. The complexes of enantiopure chiral ligands necessarily crystallize in non-centrosymmetric space groups, fulfilling one of the requirements for nonlinear optical behaviour (Masse *et al.*, 1999; Muthuraman *et al.*, 1999).

References

Allen, F. H., Kennard, O., Watson, D. G., Brammer, L., Orpen, A. G. & Taylor, R. (1987). *J. Chem. Soc. Perkin Trans. 2*, pp. S1–S19.

Arranz Mascarós, P., Cobo Domingo, J., Godino Salido, M., Gutiérrez Valero, M. D., López Garzón, R. & Low, J. N. (2000). *Acta Cryst.* C**56**, e4–e5.

Arranz Mascarós, P., Godino, M. L., López, R., Cuesta, R., Valenzuela Calahorro, C. & Martín Ramos, D. (1999). *Acta Cryst.* C**55**, 2049–2051.

Batten, S. R. & Robson, R. (1998). *Angew. Chem. Int. Ed.* **37**, 1460–1494.

Bauer, S. H. & Andreassen, A. L. (1972). *J. Phys. Chem.* **76**, 3099–3108.

Bernstein, J., Davis, R. E., Shimoni, L. & Chang, N.-L. (1995). *Angew. Chem. Int. Ed. Engl.* **34**, 1555–1573.

Davis, M. I., Boggs, J. E., Coffey, D. & Hanson, H. P. (1965). *J. Phys. Chem.* **69**, 3727–3730.

Domasevich, K. V., Gerasimchuk, N. N., Rusanov, E. B. & Gerasimchuk, O. A. (1996). *Zh. Obshch. Khim.* **66**, 652–657.

Domasevich, K. V., Mokhir, A. A. & Rusanov, E. B. (1996). *Zh. Obshch. Khim.* **66**, 1501–1505.

Domasevitch, K. V., Ponomareva, V. V. & Rusanov, E. B. (1997). *J. Chem. Soc. Dalton Trans.* pp. 1177–1180.

Domasevitch, K. V., Ponomareva, V. V., Rusanov, E. B., Gelbrich, T., Sieler, J. & Skopenko, V. V. (1998). *Inorg. Chim. Acta*, **268**, 93–101.

Ferguson, G. (1999). *PRPKAPPA*. University of Guelph, Canada.

Flack, H. D. (1983). *Acta Cryst.* A**39**, 876–881.

Gilli, P., Bertolasi, V., Ferretti, V. & Gilli, G. (1994). *J. Am. Chem. Soc.* **116**, 909–915.

Glidewell, C., Low, J. N., Arranz Mascarós, P., Cuesta Martos, R. & Gutiérrez Valero, M. D. (2002). *Acta Cryst.* C**58**, *m*61–*m*64.

Low, J. N., Arranz, P., Cobo, J., Fontecha, M. A., Godino, M. L., López, R., Cannon, D., Quesada, A. & Glidewell, C. (2001). *Acta Cryst.* C**57**, 680–682.

Low, J. N., Arranz, P., Cobo, J., Fontecha, M. A., Godino, M. L., López, R. & Glidewell, C. (2001). *Acta Cryst.* C**57**, 534–537.

Low, J. N., López, M. D., Arranz Mascarós, P., Cobo Domingo, J., Godino, M. L., López Garzón, R., Gutiérrez, M. D., Melguizo, M., Ferguson, G. & Glidewell, C. (2000). *Acta Cryst.* B**56**, 882–892.

Low, J. N., Moreno Sánchez, J. M., Arranz Mascarós, P., Godino Salido, M. L., López Garzón, R., Cobo Domingo, J. & Glidewell, C. (2001). *Acta Cryst.* B**57**, 317–328.

Masse, R., Nicoud, J.-F., Bagieu-Beucher, M. & Bourgogne, C. (1999). *Chem. Phys.* **245**, 365–375.

Muthuraman, M., Bagieu-Beucher, M., Masse, R., Nicoud, J.-F. & Desiraju, G. R. (1999). *J. Mater. Chem.* **9**, 1471–1474.

Nonius (1997). *Kappa-CCD Server Software*, Windows 3.11 Version. Nonius BV, Delft, The Netherlands.

Otwinowski, Z. & Minor, W. (1997). *Methods Enzymol.* **276**, 307–326.

Raston, C. L., Sharma, R. P., Skelton, B. W. & White, A. H. (1978). *Aust. J. Chem.* **31**, 745–755.

Schlemper, E. O., Murmann, R. K. & Hussain, M. S. (1986). *Acta Cryst.* C**42**, 1739–1743.

Shannon, R. D. & Prewitt, C. T. (1970). *Acta Cryst.* B**26**, 1046–1048.

Sheldrick, G. M. (1997*a*). *SHELXS*97. University of Göttingen, Germany.

Sheldrick, G. M. (1997*b*). *SHELXL*97. University of Göttingen, Germany.

Spek, A. L. (2003). *J. Appl.Cryst.* **36**, 7–13.

Starbuck, J., Norman, N. C. & Orpen, A. G. (1999). *New J. Chem.* **23**, 969–972.

Talberg, H. J. (1977). *Acta Chem. Scand. A*, **31**, 485–491.

Wilson, A. J. C. (1976). *Acta Cryst.* A**32**, 994–996.